J. Fluid Mech. (2013), *vol.* 718, *pp.* 428–456. © Cambridge University Press 2013
doi:10.1017/jfm.2012.619

Longwave Marangoni convection in a surfactant solution between poorly conducting boundaries

Sergey Shklyaev[1,2,†] **and Alexander A. Nepomnyashchy**[3,4]

[1]Department of Chemical Engineering, University of Puerto Rico – Mayagüez, Mayagüez, PR 00681, USA

[2]Institute of Continuous Media Mechanics, Ural Branch of Russian Academy of Sciences, Perm 614013, Russia

[3]Department of Mathematics, Technion – Israel Institute of Technology, Haifa 32000, Israel

[4]Minerva Center for Nonlinear Physics of Complex Systems, Technion – Israel Institute of Technology, Haifa 32000, Israel

(Received 18 July 2011; revised 3 December 2012; accepted 11 December 2012; first published online 8 February 2013)

We consider Marangoni convection in a heated layer of a binary liquid. The solute is a surfactant, which is present in both surface and bulk phases; the bulk gradient of the concentration is formed due to the Soret effect. Linear stability analysis demonstrates a well-pronounced stabilization of the layer due to the adsorption kinetics and advection of the surface phase. We derive nonlinear amplitude equations for longwave perturbations in the case of fast sorption kinetics (small Langmuir number) and demonstrate that with increase in the effect of the adsorption, subcritical excitation occurs. In the case of a finite Langmuir number, the weakly nonlinear problem is ill-posed. A physical mechanism of subcritical bifurcation is discussed.

Key words: Marangoni convection, pattern formation, thin films

1. Introduction

The investigation of the surfactant dynamics is important due to numerous applications in medicine, chemistry and engineering. Well-developed experimental techniques (Li *et al.* 1993; Penfold *et al.* 1997; Raina, Kulkarni & Rao 2001) as well as modern numerical methods of molecular dynamics type (Tarek, Bandyopadhyay & Klein 1998; Shin & Abbott 2001; Andoh & Yasuoka 2007) allow a detailed study of the microscopic processes near an interface and/or a free surface. Another efficient and far-reaching way of treating liquids with surface active agents is the macroscopic description within the phenomenological models (Levich 1962; Landau & Lifshitz 1987; Leal 2007). Interaction of several kinetic processes (e.g. heat and/or mass transfer in a bulk, a surface diffusion, sorption processes), with various characteristic time scales, makes this problem intricate and potentially rich in dynamical aspects (Edmonstone, Matar & Craster 2006; Craster & Matar 2009; Matar & Craster 2009; Yiantsios & Higgins 2010).

† Email address for correspondence: shklyaev@yandex.ru

https://doi.org/10.1017/jfm.2012.619 Published online by Cambridge University Press

The influence of the surfactant on the thermocapillary convection was studied by many authors. Within the linear stability theory, the problem was first considered by Berg & Acrivos (1965) and Vidal & Acrivos (1966), where a significant increase in the stability threshold for the monotonic mode was found. Later, Palmer & Berg (1972) revealed that in fact there is no strong stabilization of a quiescent state, because an oscillatory mode becomes critical. The impacts of the surface deformation (Ryabitskii 1993), adsorption/desorption kinetics for a soluble surfactant (Ryabitskii 1996) and the Soret effect (Ryabitskii 2000) were addressed. It should be noted that similarly to the paper by Scriven & Sternling (1964) the gravity is completely disregarded in these papers, which results in a zero critical Marangoni number for the longwave mode irrespectively of the presence of the surfactant (this unlikely effect disappears under the gravity, see Smith (1966)). In a series of papers by Nepomnyashchy & Simanovskii (1986, 1988, 1992) the same effects were studied for a two-layer system.

Most experimental studies show that a characteristic time of a sorption process is relatively small in comparison with a typical convective time scale (MacLeod & Radke 1994; Johnson & Stebe 1996; Lin, Lu & Hwang 1996). Thus, the adsorption/desorption kinetics can be safely neglected for such systems. However, in a number of experimental works (see, for instance, Pan, Green & Maldarelli (1998) and the survey by Kumar, Couzis & Maldarelli (2003)), the typical time of desorption is found to be large enough and, therefore, competition between diffusive mass transfer and sorption kinetics certainly occurs. Moreover, recent experiments (Kostarev, Zuev & Viviani 2009) clearly demonstrate that adsorption kinetics is of crucial importance in solutocapillary convection, leading to a substantial delay in an intensive convective motion. Therefore, further studies in this field are motivated.

The mentioned theoretical papers (Berg & Acrivos 1965; Vidal & Acrivos 1966; Palmer & Berg 1972; Ryabitskii 1993, 1996, 2000) on a single-layer system were devoted to the case of a substrate of large thermal conductivity. The analysis in the opposite case of the thermal boundary condition, a poorly conductive substrate, has been carried out only for the simplest case of insoluble surfactant (Mikishev & Nepomnyashchy 2010*a*,*b*; Hamid, Kechil & Aziz 2011). Generalization of the above studies to the case of a soluble surfactant can be interesting. Indeed, in the case of a nearly insulated layer of a binary solution both monotonic and oscillatory longwave modes were found by Oron & Nepomnyashchy (2004). The oscillatory mode demonstrates a complicated dynamics, when both alternating rolls on a square lattice (Shklyaev, Nepomnyashchy & Oron 2007) and a three-parameter family of solutions on a hexagonal lattice are selected (Shklyaev, Nepomnyashchy & Oron 2009*a*, 2011). In the latter case, a heteroclinic cycle emerges under certain conditions. It should be emphasized that according to Shklyaev *et al.* (2011), both square and hexagonal wavy patterns can be stable simultaneously on a superlattice, which combines these two lattices.

Despite the above-mentioned progress, the longwave oscillatory mode is a rare and still not sufficiently studied subject. One of the principal points of the model used in previous researches in this field is that the mean concentration does not influence the dynamics, therefore only the gradients of amplitude functions, rather than the functions themselves, enter into the amplitude equations. This simplifies the nonlinear analysis to a great extent, but there are many problems, where such simplification fails. Adsorption kinetics provides an example of such a problem, which is the main motivation of the present work. Among the other similar problems, with their specific amplitude functions, the convection in systems with a deformable free

https://doi.org/10.1017/jfm.2012.619 Published online by Cambridge University Press

surface (interface) and/or with non-Boussinesq effects can be mentioned. The small non-Boussinesq effects were considered in some particular case by Pismen (1988).

The paper addresses instabilities in a heated liquid layer containing a soluble surfactant, which is present in both bulk and surface phases. Both linear stability and weakly nonlinear dynamics are studied. The results of the investigation differ significantly from those obtained formerly in the absence of a solute adsorption at the interface (Oron & Nepomnyashchy 2004; Shklyaev *et al.* 2007, 2009*a*, 2011). The paper is organized as follows: we formulate the problem in § 2. In § 3 the linear stability problem is analysed for both longwave and shortwave perturbations. Then, § 4 focuses on the nonlinear dynamics; first we treat the limiting case of fast sorption kinetics in § 4.1 for the monotonic mode and in §§ 4.2 and 4.3 for the oscillatory mode. The analysis of the general case is carried out in § 4.4, which results in an ill-posed set of equations. We draw conclusions in § 5.

2. Governing equations

We consider a layer of a binary mixture heated from below; a constant transverse gradient of the temperature $-a$ is specified at the boundary with the rigid substrate $z = 0$. It is well known that in the case of a pure liquid there are two basic types of Marangoni instabilities: (i) the development of a cellular convection with a negligible surface deformation (Pearson 1958); and (ii) the deformational instability leading typically to a rupture of the layer (Smith 1966). Historically the latter mode was revealed by Scriven & Sternling (1964), but due to neglecting the gravity the authors obtained instability for infinitesimal heating. While the former type of the instability is ubiquitous, the latter type can take place only in very thin films (VanHook *et al.* 1997). Both types of instabilities are clearly distinguishable also in the case of a binary mixture (Podolny, Oron & Nepomnyashchy 2005, 2006).

In the present paper, we consider only the former type of instabilities. Therefore, it is assumed that the upper boundary $z = d$ is free and non-deformable. This assumption is valid in a moderately thin layer, i.e. the gravity is large, $Ga = gd^3/\nu^2 \gg 1$, but not too large, $Gr = g\beta a d^4/\nu^2 \ll 1$, to prevent the emergence of buoyancy convection, where ν is the kinematic viscosity and β is the thermal expansion coefficient. For instance, under terrestrial conditions these inequalities are met for a water layer of $d \sim 0.01$–0.1 cm.

The heat flux from the surface is governed by Newton's law of cooling. The solute is a soluble surfactant, i.e. it is present in two phases: a surface one (with the surface concentration Γ) and a bulk one (with the bulk concentration C). We take the Soret effect into account, which under the condition of a zero net flux of the surfactant leads to formation of the bulk concentration gradient across the layer. The sorption kinetics ensures a surfactant exchange between the phases according to the following relations valid at the free surface:

$$D\,(C + \alpha_D T)_z = -k_a C + k_d \Gamma, \tag{2.1}$$

$$\Gamma_t + \nabla_2 \cdot (\Gamma \boldsymbol{u}) = D_s \nabla_2^2 \Gamma + k_a C - k_d \Gamma. \tag{2.2}$$

Hereafter a subscript denotes a partial derivative with respect to a corresponding variable; $\boldsymbol{u}$ and ∇_2 are the two-dimensional projections of the velocity and gradient onto the x–y plane, respectively, α_D, D, D_s, k_a and k_d are the Soret coefficient, bulk and surface diffusion coefficients of the surfactant, adsorption and desorption rates, respectively.

https://doi.org/10.1017/jfm.2012.619 Published online by Cambridge University Press

The surface tension linearly depends on both the temperature and the surface concentration of the surfactant:

$$\sigma = \sigma_* - \sigma_T(T - T_*) - \sigma_\Gamma(\Gamma - \Gamma_*), \tag{2.3}$$

where the asterisks in the subscripts denote the reference values of the corresponding quantities; σ_* and T_* are unimportant for the further analysis, Γ_* is discussed below. This variation of the surface tension gives rise to the tangential stress according to the following expression:

$$\eta \boldsymbol{u}_z = -\boldsymbol{\nabla}_2(\sigma_T T + \sigma_\Gamma \Gamma). \tag{2.4}$$

Here η is the dynamic viscosity.

We choose d, d^2/κ, κ/d, $\eta\kappa/d^2$, ad, $\sigma_\Gamma^{-1}\sigma_T ad$, $k_d\sigma_T ad(k_a\sigma_\Gamma)^{-1}$ (κ is the thermal diffusivity), as the reference values for length, time, velocity, pressure, temperature, surface and bulk concentration, respectively. (The bulk concentration C, which is defined as the mass fraction, is a dimensionless variable, but its rescaling in the above-mentioned manner simplifies the analysis and the comparison with the previous works.) With this choice of units we arrive at the following boundary value problem

$$\frac{1}{P}(\boldsymbol{v}_t + \boldsymbol{v}\cdot\boldsymbol{\nabla}\boldsymbol{v}) = -\boldsymbol{\nabla}p + \nabla^2\boldsymbol{v}, \tag{2.5a}$$

$$T_t + \boldsymbol{v}\cdot\boldsymbol{\nabla}T = \nabla^2 T, \tag{2.5b}$$

$$\frac{1}{L}(C_t + \boldsymbol{v}\cdot\boldsymbol{\nabla}C) = \nabla^2 C + \chi\nabla^2 T, \tag{2.5c}$$

$$\boldsymbol{\nabla}\cdot\boldsymbol{v} = 0; \tag{2.5d}$$

$$\boldsymbol{v} = 0, \quad T_z = -1, \quad C_z + \chi T_z = 0 \quad \text{at } z = 0, \tag{2.6a}$$

$$\begin{gathered} w = 0, \quad C_z + \chi T_z + \frac{K_a}{L}(C - \Gamma) = 0, \quad \boldsymbol{u}_z = -M\boldsymbol{\nabla}_2(T + \Gamma), \\ C - \Gamma = K_d^{-1}[\Gamma_t + \boldsymbol{\nabla}_2\cdot(\Gamma\boldsymbol{u}) - L_s\nabla_2^2\Gamma], \quad T_z = -BT \quad \text{at } z = 1, \end{gathered} \tag{2.6b}$$

where w is the z-component of the velocity.

The boundary-value problem (2.5) and (2.6) is characterized by eight dimensionless parameters. Five of them,

$$P = \frac{\nu}{\kappa}, \quad L = \frac{D}{\kappa}, \quad B = \frac{qd}{k_{th}}, \quad M = \frac{\sigma_T a d^2}{\eta\kappa}, \quad \chi = \frac{\alpha_D k_a \sigma_\Gamma}{k_d \sigma_T} \tag{2.7}$$

are the Prandtl, Lewis, Biot, Marangoni and Soret numbers, respectively; the same parameters control the problem in the absence of the adsorption/desorption kinetics (Oron & Nepomnyashchy 2004). (Here k_{th} is the heat conductivity and q is the heat transfer coefficient in Newton's law of cooling.) These parameters, except for the last one, are defined in the same manner as in the cited paper. The sign of χ is chosen in the opposite way to that by Oron & Nepomnyashchy (2004), since in the cited paper positive σ_C stands for the aqueous solution of inorganic salt, when the surface tension increases with growth of C. In the case under consideration, $\sigma_\Gamma > 0$ means that the surface tension decreases with the growth of Γ, which is inherent to surfactant.

The remaining three parameters characterize the adsorption/desorption kinetics and diffusion of the adsorbed surfactant:

$$K_a = \frac{k_a d}{\kappa}, \quad K_d = \frac{k_d d^2}{\kappa}, \quad L_s = \frac{D_s}{\kappa}. \tag{2.8}$$

https://doi.org/10.1017/jfm.2012.619 Published online by Cambridge University Press

They are the dimensionless adsorption and desorption coefficients and the surface Lewis number, respectively. It is worth noting, that K_d^{-1} plays the role of the characteristic non-dimensional time of the equilibration between the phases. If $K_d^{-1} \to 0$ the bulk and surface phases are in the local equilibrium, $C(z=1) = \Gamma$, i.e. the problem reduces to that studied by Oron & Nepomnyashchy (2004). (Below we term this limiting case 'infinitely fast kinetics' or 'absence of the adsorption'.) In the opposite limit, $K_d \ll 1$, the surfactant is insoluble; in this case the volume concentration C is irrelevant. That limit of the problem was investigated by Mikishev & Nepomnyashchy (2010*a*,*b*) and Hamid *et al.* (2011).

Note, that upon elimination of $C - \Gamma$ from the mass balance condition at $z = 1$, one readily obtains

$$(C + \chi T)_z = -\frac{K_{ad}}{L}[\Gamma_t + \nabla_2 \cdot (\Gamma \boldsymbol{u}) - L_s \nabla^2 \Gamma], \tag{2.9}$$

where parameter $K_{ad} = K_a K_d^{-1} = k_a/(k_d d)$, that will be called the Langmuir number, is a dimensionless ratio of the adsorption and desorption coefficients.

The boundary-value problem (2.5) and (2.6) admits an equilibrium base state, corresponding to the conductive distributions of both the temperature and bulk concentration in the quiescent liquid:

$$\boldsymbol{v}_0 = 0, \quad T_0 = -z + \frac{B+1}{B}, \quad C_0 = \langle C \rangle + \chi\left(z - \frac{1}{2}\right), \quad \Gamma_0 = \langle C \rangle + \frac{1}{2}\chi; \tag{2.10}$$

where $\langle C \rangle$ is the scaled mean value of the bulk concentration. In this state, the desorption is exactly balanced by the adsorption. Below we study the stability of the base state with respect to small perturbations and nonlinear evolution of disturbances.

The reference value of Γ_0, the dimensionless value of Γ_*, which appears in (2.3), is the ninth dimensionless parameter governing the dynamics of the system. Another candidate for being the ninth parameter is the mean value of the bulk concentration $\langle C \rangle$. However, both of these parameters include the temperature gradient a via the scales for the surface and volume concentrations; thus, they are inconvenient from the experimental point of view, since when varying the layer heating one varies both Γ_0 and $\langle C \rangle$ as well. Therefore, an optimal choice of the ninth parameter is the so-called elasticity number:

$$N = M\langle C \rangle = \frac{\sigma_\Gamma k_a \langle C^{(us)} \rangle d}{k_d \eta \kappa}, \tag{2.11}$$

where $\langle C^{(us)} \rangle$ is the unscaled mean value of the bulk concentration. Nevertheless, below we also frequently use $\Gamma_0 = N/M + \chi/2$.

It is important to emphasize that for $K_d \gg 1$ (Oron & Nepomnyashchy 2004), the mean value of the bulk concentration does not influence the dynamics of the layer: only the gradient of concentration is relevant. For finite values of K_d the mean concentration is a significant parameter of the problem.

Let us briefly discuss the limitations imposed on the dimensionless parameters. First, we have to provide positive values of the surface and bulk concentrations of the surfactant $C_0 \mathrm{sgn} M$ and $\Gamma_0 \mathrm{sgn} M$. (Note that the scales for both C and Γ are chosen proportional to $\sigma_T a$ and therefore they are of the same signs as the Marangoni number.) Next, the unscaled concentration $C_0^{(us)} = C_0 k_d \sigma_T a d/(k_a \sigma_\Gamma)$ has to be less than unity. Moreover, we have neglected the dependence of the Soret coefficient on both the temperature and the concentration. Because $\alpha_D = D_T C^{(us)}(1 - C^{(us)})$, where D_T is the

https://doi.org/10.1017/jfm.2012.619 Published online by Cambridge University Press

thermal diffusion coefficient, the latter assumption can be justified, when the unscaled concentration is far from both zero and unity. Otherwise, C_0 is a nonlinear function of z (see Kalitzova-Kurteva, Slavtchev & Oron 2009; Slavtchev, Kalitzova-Kurteva & Oron 2009). For instance, if we demand that $1/4 < C_0^{(us)}(z) < 3/4$ for any z, i.e. the maximum value of $C_0^{(us)}$ does not exceed three times of its minimum value, we arrive at the inequalities

$$N > |M\chi|. \tag{2.12}$$

Below this restriction is taken into account. There also exists an additional limitation on the dimensionless group $\langle C^{(us)}\rangle$: $\langle C^{(us)}\rangle - |\alpha_D ad/2| > 1/4$. However, $\langle C^{(us)}\rangle$ does not influence the analysis presented below.

3. Linear stability analysis

Let us linearize (2.5) and (2.6) around the base state. Problem (2.5) and (2.6) is invariant with respect to rotations in the horizontal plane (x, y). Therefore, the growth rate of the instability does not depend on the direction of the wavevector $\boldsymbol{k}$. Thus, it is sufficient to consider two-dimensional normal perturbations of the form $f(x, z, t) = \hat{f}(z)\exp(\mathrm{i}kx + \lambda t)$ corresponding to a wavevector directed along the axis x. We obtain

$$\frac{\lambda}{P}\hat{u} = -\mathrm{i}k\hat{p} + \Delta\hat{u}, \tag{3.1a}$$

$$\frac{\lambda}{P}\hat{w} = -\hat{p}' + \Delta\hat{w}, \tag{3.1b}$$

$$\lambda\hat{T} - \hat{w} = \Delta\hat{T}, \tag{3.1c}$$

$$\lambda\hat{C} + \chi\hat{w} = L\Delta(\hat{C} + \chi\hat{T}), \tag{3.1d}$$

$$\mathrm{i}k\hat{u} + \hat{w}' = 0; \tag{3.1e}$$

$$\hat{u} = \hat{w} = \hat{T}' = \hat{C}' = 0 \quad \text{at } z = 0, \tag{3.2a}$$

$$\begin{gathered}\hat{w} = \hat{T}' + B\hat{T} = 0, \quad (\hat{C} + \chi\hat{T})' = -\frac{K_{ad}}{L}(\lambda\hat{\Gamma} + \Gamma_0\mathrm{i}k\hat{u} + L_s k^2\hat{\Gamma}),\\ \hat{u}' = -Mik(\hat{T} + \hat{\Gamma}), \quad \hat{C} - \hat{\Gamma} = K_d^{-1}(\lambda\hat{\Gamma} + \Gamma_0\mathrm{i}k\hat{u} + L_s k^2\hat{\Gamma}) \quad \text{at } z = 1,\end{gathered} \tag{3.2b}$$

where the prime denotes a z-derivative, $\Delta = \mathrm{d}/\mathrm{d}z^2 - k^2$ is the Fourier transform of the Laplace operator. The eigenvalue problem (3.1)–(3.2) is not self-adjoint. The eigenvalues λ can be either real or form complex-conjugate pairs.

For most binary liquids the Lewis number is rather small, although we do not treat it to be asymptotically small, setting $L = 0.01$ in calculations. Analysis of asymptotically small L can be found in Shklyaev, Nepomnyashchy & Oron (2009*b*) and Shklyaev & Nepomnyashchy (2011) for infinite and finite values of the Langmuir number K_d, respectively. The available results of measurements for D_s are somewhat controversial. The majority of authors (see Agrawal & Neuman 1988) found that the surface diffusion was smaller than the bulk one, an opposite conclusion was reported by Valkovska & Danov (2000). Hereafter we assume $L_s = 0$ in numerical calculations, although we retain it in analytical formulas. In fact, setting $L_s \sim L$ does not change the numerical results substantially.

Finally, let us estimate the typical values of parameters K_a and K_d governing the sorption kinetics. For 1-decanol the desorption time is small enough, $k_d = 10$–$100\ \mathrm{s}^{-1}$

https://doi.org/10.1017/jfm.2012.619 Published online by Cambridge University Press

depending on the concentration of the surfactant. This provides $K_d = 10^4$–10^5 for a 1 cm layer, i.e. the sorption kinetics serves only as a weak effect (however, it can still be important, see §§ 4.1–4.3). For polyethoxylated surfactants the adsorption and desorption are very slow processes, $k_d \sim 10^{-4}$ s^{-1}, $k_a \sim 10^{-3}$ cm s^{-1} (Pan *et al.* 1998), which results in $K_d \sim 0.1$ and $K_a \sim 1$. Therefore, below we analyse both cases of finite K_a and K_d and the limit of fast kinetics, $K_{ad} \ll 1$.

3.1. *Longwave instability*

In the present paper, we consider the case of poorly conducting boundaries, i.e. $B \ll 1$. As shown by Pearson (1958), in the latter case the instability is characterized by the scaling $k \sim B^{1/4}$, i.e. a longwave instability takes place. In the case of the binary liquid, there are two different characteristic wavenumber scales of a longwave instability, $k \sim B^{1/4}$ (Oron & Nepomnyashchy 2004) and $k \sim B^{1/2}$ (Podolny *et al.* 2005). In the present section, we consider the former interval of wavenumbers; the latter region will be considered in § 3.2. It is convenient to define a new small parameter ϵ connected with B by the relation

$$B = \epsilon^4. \tag{3.3}$$

Then the wavenumber and the growth rate are scaled in the following way:

$$k = \epsilon K, \quad \lambda = \epsilon^2 \Lambda, \tag{3.4}$$

and the fields of perturbations, the Marangoni number and the growth rate are expanded as follows:

$$\hat{T} = \hat{T}_0 + \epsilon^2 \hat{T}_2 + \cdots, \quad \hat{C} = \hat{C}_0 + \epsilon^2 \hat{C}_2 + \cdots, \tag{3.5a}$$

$$\hat{p} = \hat{p}_0 + \epsilon^2 \hat{p}_2 + \cdots, \quad \hat{u} = \epsilon(\hat{u}_0 + \epsilon^2 \hat{u}_2 + \cdots), \quad \hat{w} = \epsilon^2(\hat{w}_0 + \epsilon^2 \hat{w}_2 + \cdots), \tag{3.5b}$$

$$M = M_0 + \epsilon^2 M_2 + \cdots \quad \Lambda = \Lambda_0 + \epsilon^2 \Lambda_2 + \cdots. \tag{3.5c}$$

Substituting these expansions into (3.1) and (3.2), we collect the terms of the same order in ϵ^2.

The zeroth-order problem has the form

$$\hat{T}_0'' = 0, \quad \hat{C}_0'' = 0, \tag{3.6a}$$

$$\hat{p}_0' = 0, \quad \hat{u}_0'' = \mathrm{i}K\hat{p}_0, \quad \mathrm{i}K\hat{u}_0 + \hat{w}_0' = 0, \tag{3.6b}$$

$$\hat{u}_0 = \hat{w}_0 = \hat{T}_0' = \hat{C}_0' = 0 \quad \text{at } z = 0, \tag{3.6c}$$

$$\hat{w}_0 = \hat{T}_0' = \hat{C}_0' = \hat{C}_0 - \hat{\Gamma}_0 = 0, \quad \hat{u}_0' = -\mathrm{i}KM_0(\hat{T}_0 + \hat{\Gamma}_0) \quad \text{at } z = 1. \tag{3.6d}$$

This problem has an obvious solution

$$\hat{T}_0 = F, \quad \hat{C}_0 = \hat{\Gamma}_0 = G, \quad \hat{p}_0 = -\frac{3M_0}{2}(F + G), \tag{3.7}$$

$$\hat{u}_0 = \frac{M_0}{4}\mathrm{i}K(F + G)(2z - 3z^2), \tag{3.8}$$

$$\hat{w}_0 = -\frac{M_0}{4}K^2(F + G)(z^3 - z^2). \tag{3.9}$$

In the second order with respect to ϵ we need only the heat and mass balance equations:

$$\hat{T}_2'' = (\Lambda_0 + K^2)\hat{T}_0 - \hat{w}_0, \tag{3.10a}$$

https://doi.org/10.1017/jfm.2012.619 Published online by Cambridge University Press

$$\hat{C}_2'' + \chi \hat{T}_2'' = \left(\frac{\Lambda_0}{L} + K^2 \right) \hat{C}_0 + \frac{\chi}{L} \hat{w}_0 + \chi K^2 \hat{T}_0, \tag{3.10b}$$

$$\hat{T}_2' = \hat{C}_2' = 0 \quad \text{at } z = 0, \tag{3.10c}$$

$$\hat{C}_2' = -\frac{K_{ad}}{L} [(\Lambda_0 + L_s K^2) \hat{\Gamma}_0 + \mathrm{i} K \Gamma_0 \hat{u}_0], \quad \hat{T}_2' = 0 \quad \text{at } z = 1. \tag{3.10d}$$

The solvability condition for (3.10) results in

$$\Lambda_0^2 (1 + K_{ad}) + a_1 \Lambda_0 K^2 + a_2 K^4 = 0, \tag{3.11}$$

where

$$a_1 = 1 + L + K_{ad} \left(1 + L_s + \frac{N}{4} \right) - m_0 [1 - \chi + K_{ad} (1 - 6\chi)], \tag{3.12}$$

$$a_2 = L + K_{ad} \left(L_s + \frac{N}{4} \right) - m_0 [L - \chi - \chi L + K_{ad} (L_s - 6\chi)], \tag{3.13}$$

and $m_0 = M_0/48$. (Here we have taken into account that $\Gamma_0 = N/M_0 + \chi/2$.)

Equation (3.11) describes both the monotonic and oscillatory modes. For the monotonic mode the stability threshold is given by

$$m_*^{(m)} = \frac{L + K_{ad}(L_s + N/4)}{L - \chi - \chi L + K_{ad}(L_s - 6\chi)}. \tag{3.14}$$

The critical value $\chi_{m\infty}$, corresponding to infinite value of $m_*^{(m)}$, is as follows

$$\chi_{m\infty} = \frac{L + K_{ad} L_s}{1 + L + 6K_{ad}}. \tag{3.15}$$

For the oscillatory mode the stability threshold is given by

$$m_*^{(o)} = \frac{1 + L + K_{ad}(1 + L_s + N/4)}{1 - \chi + K_{ad}(1 - 6\chi)}. \tag{3.16}$$

The latter mode takes place, when the squared frequency of perturbations

$$\Omega^2 = K^4 \left(1 - \frac{m_*^{(o)}}{m_*^{(m)}} \right) \frac{L + K_{ad}(L_s + N/4)}{1 + K_{ad}} \tag{3.17}$$

is positive. After simple calculations this condition can be rewritten as

$$\chi_{o\infty} > \chi > \chi_0, \tag{3.18}$$

where

$$\chi_0 = \frac{L^2 + K_{ad}(2LL_s - (1 - L)N/4) + K_{ad}^2 (L_s^2 - (1 - L_s)N/4)}{1 + L + L^2 + K_{ad}(7 + L(1 + L_s + N/4)) + 6K_{ad}^2} \tag{3.19}$$

and $\chi = \chi_{o\infty}$ is the vertical asymptote for $m_*^{(o)}(\chi)$ determined by

$$\chi_{o\infty} = \frac{1 + K_{ad}}{1 + 6K_{ad}}. \tag{3.20}$$

It is worth noting that (3.14) and (3.16) match both known limiting cases, infinitely fast kinetics, $K_{ad} = 0$ (Oron & Nepomnyashchy 2004) and insoluble surfactant, $K_{ad} \gg 1$, $\chi = 0$ (Mikishev & Nepomnyashchy 2010*a*).

https://doi.org/10.1017/jfm.2012.619 Published online by Cambridge University Press

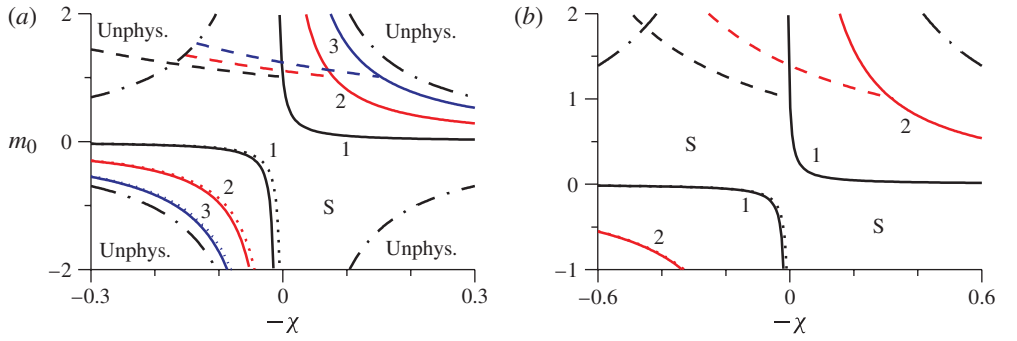


FIGURE 1. (Colour online) Critical Marangoni number m_0 for the longwave modes at $L_s = 0$, $L = 0.01$: (*a*) $N = 10$ and (*b*) $N = 40$. Lines 1–3 correspond to the Langmuir number, K_{ad}, being equal to 0, 0.04, 0.1, respectively. The solid lines show the stability boundaries for the monotonic mode, (3.14), the dashed and dotted lines are for the oscillatory mode, (3.16), and monotonic mode with $k = O(\sqrt{B})$, (3.26), respectively. Domains of stability are marked 'S'. For positive (negative) m_0 the condition (2.12) is violated above (below) the dot-dashed lines; these unphysical domains are marked 'unphys'.

Results of the computation are presented in figure 1. The dependence $m_0(\chi)$ is typical for a Soret-driven convection in binary mixtures (Chen & Chen 1994; Oron & Nepomnyashchy 2004), see also variation of the critical Rayleigh number with the Soret number for a buoyancy convection (Hurle & Jakeman 1971). The increase in both N and K_{ad} leads to a well-pronounced stabilization, $|m_*|$ increases for both the monotonic and oscillatory modes.

Proceeding with the expansion for the monotonic mode to the second-order with respect to ϵ^2, one can readily obtain the correction to the Marangoni number:

$$m_2 = m_*^{(m)} \left(\frac{f_\beta}{K^2} + f_K K^2 \right), \tag{3.21}$$

where

$$f_\beta = \frac{K_{ad} L_s + L - \chi L}{L - \chi - \chi L + K_{ad}(L_s - 6\chi)}, \tag{3.22a}$$

$$f_K = \frac{q_1 + q_2 L K_d^{-1}}{15(L - \chi - \chi L + K_{ad}(L_s - 6\chi))(L + K_{ad}(L_s + N/4))}, \tag{3.22b}$$

$$q_1 = L^2(1 - \chi) - \chi L + K_{ad}\,[24\chi L - L_s(6\chi(1 + L) - 2L) - 5(\chi L - L + \chi)N/4] + K_{ad}^2 L_s(L_s - 6\chi), \tag{3.22c}$$

$$q_2 = 15(6\chi L - \chi(1 + L)(L_s + N/4) + LN/4). \tag{3.22d}$$

Thus, returning back to the unscaled wavenumber k and Biot number B, we obtain the marginal stability curve for the monotonic mode:

$$M_* \approx 48 m_*^{(m)} \left(1 + f_\beta \frac{B}{k^2} + f_K k^2 \right). \tag{3.23}$$

It can be shown that for $L = 0.01$, $L_s = 0$, $f_K > 0$ at $N > 0.3$ and arbitrary values of the Soret and Langmuir numbers. At $N < 0.3$, which is compatible with (2.12)

https://doi.org/10.1017/jfm.2012.619 Published online by Cambridge University Press

only for extremely small $|\chi|$, the longwave analysis is not sufficient; below we do not consider this parameter range.

It is clear that $f_\beta > 0$ when $\chi < \chi_{m\infty}$ or $\chi > \chi_1$, where $\chi_1 = 1 + K_{ad}L_s/L > \chi_{m\infty}$, and f_β is negative otherwise. In the latter case the conventional scaling, $B = O(k^4)$, becomes inappropriate (Podolny *et al.* 2005). We consider this case in § 3.2.

3.2. *Longwave mode with* $k = O(\sqrt{B})$

As has been shown for $K_{ad} = 0$ by Podolny *et al.* (2005), when $f_\beta < 0$ in (3.23), the analysis of the wavenumber interval $k \sim B^{1/4}$ is not sufficient, and it is also necessary to investigate the growth rate for smaller wavenumbers, $k \sim B^{1/2}$. Later on, we define

$$B = \bar{\epsilon}^2. \tag{3.24}$$

The corresponding mode is critical for a heating from above only. Here we generalize the results of the cited paper to the case of the finite Langmuir number K_{ad}.

The rescaling from (3.3) to (3.24) keeps (3.6)–(3.10) unchanged with the only exception $\hat{T}_2' = -\hat{T}_0$ at $z = 1$ now.

Generalization of (3.11) is straightforward; it can be easily shown that for the oscillatory mode this scaling leads to a stabilization for finite K, whereas the stability threshold for $K \gg 1$ is given by (3.16). For the monotonic mode one can obtain

$$m_*^{(\beta)} = \frac{(L + K_{ad}(L_s + N/4))\beta_K}{L - \chi\beta_K - \chi L + K_{ad}\,(L_s - 6\chi\beta_K)}. \tag{3.25}$$

Here $\beta_K = 1 + K^{-2}$.

Within the interval $\chi_1 > \chi > \chi_{m\infty}$, $m_*^{(\beta)}$ decreases monotonically from

$$m_*^{(l)} = -\frac{L + K_{ad}(L_s + N/4)}{\chi(1 + 6K_{ad})} \tag{3.26}$$

at $K = 0$ to $m_*^{(m)}$ at $K \gg 1$; therefore, $m_*^{(l)}$ materializes the critical Marangoni number. Within the interval $\chi_{m\infty} > \chi > 0$ the maximum (critical) value of $m_*^{(\beta)}$ is still given by (3.26), whereas at a certain value K_* of the wavenumber $m_*^{(\beta)}$ diverges and at $K > K_*$ there is no instability for heating from above.

Therefore, for $\chi_1 > \chi > 0$ the critical perturbations are genuine longwave ones (with $K = 0$) and the stability threshold is given by (3.26). The corresponding stability boundaries are shown in figure 1 by the dotted lines.

3.3. *Shortwave modes*

The neutral stability curve $M_*(k)$ can be readily obtained for the monotonic mode at arbitrary values of k. However, the final expression is too cumbersome and therefore it is not presented here. The examples of computations are shown in figure 2, where we choose $\chi < 0$, $\chi_{m\infty} > \chi > 0$ and $\chi_1 > \chi > \chi_{m\infty}$ for panels (*a*)–(*c*), respectively.

In the first case the marginal stability curves for both $B = 0$ and $B = 0.01$ agree well with the conventional longwave asymptotics, see (3.23). For the remaining values of χ, the longwave asymptotics with $k = O(\sqrt{B})$ for heating from above is appropriate: the minimum value of $-M_*(k)$ is materialized exactly at $k = 0$ and the stability threshold for $B = 0$ is either above that for non-zero B or even becomes infinite, see figures 2(*c*) and 2(*b*), respectively.

Shortwave oscillatory mode for $K_d^{-1} = 0$ was found by Shklyaev *et al.* (2009*b*); this mode is critical for $\chi > \chi_*$, where χ_* slightly varies with B around the value 0.1. However, the sorption kinetics strongly damps the shortwave oscillatory perturbations.

https://doi.org/10.1017/jfm.2012.619 Published online by Cambridge University Press

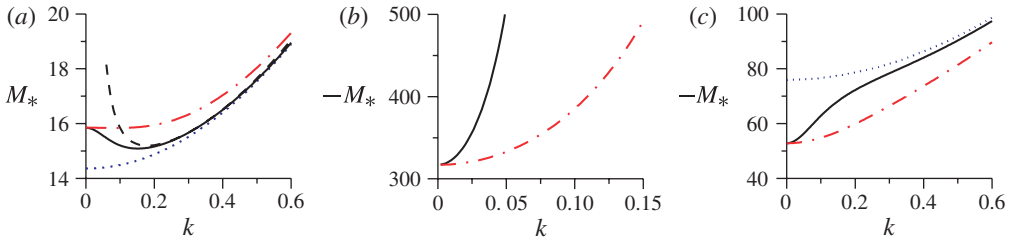


FIGURE 2. (Colour online) Marginal stability curves $M_*(k)$ for the monotonic mode at $L = 0.01, L_s = 0, K_{ad} = 0.01, K_d = 1, N = 10$: (*a*) $\chi = -0.1$; (*b*) $\chi = 0.005$; (*c*) $\chi = 0.03$. The dotted, solid and dot-dashed lines correspond to $B = 0$, $B = 0.01$ and $B = 0.1$, respectively. The dashed line in (*a*) shows the conventional longwave asymptotics (3.23) for $B = 0.01$. Domains of stability are situated below the lines.

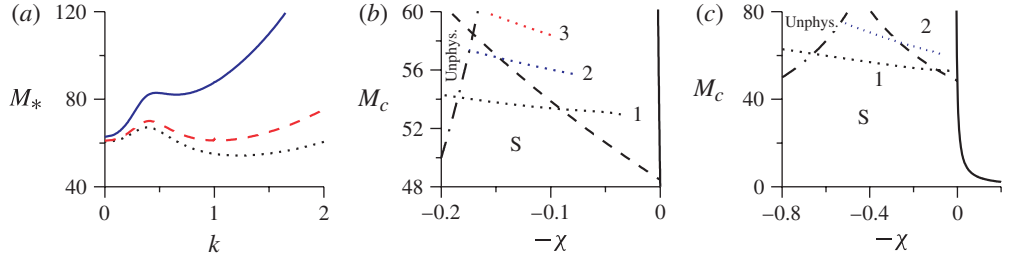


FIGURE 3. (Colour online) Linear stability for the shortwave oscillatory mode. (*a*) Marginal stability curves $M_*(k)$ at $\chi = 0.2, L = 0.01, L_s = 0, N = 10, K_a = 1, B = 0$. The dotted, solid, dashed lines correspond to $K_d^{-1} = 0, 0.002, 0.01$, respectively. The stability domain is situated below the lines. (*b,c*) Critical Marangoni number M_c for $L_s = 0, L = 0.01, K_a = 1, B = 0$: (*b*) $N = 10$ and (*c*) $N = 40$. Lines 1–3 correspond to $K_d^{-1} = 0, 0.001, 0.002$, respectively. The dotted lines depict the shortwave oscillatory mode, the solid (dashed) lines indicate the stability boundaries for the monotonic (oscillatory) longwave mode for $K_d \to \infty$. (The corresponding curves for finite K_d cannot be distinguished from those on the scale of the figures.) Domains of stability are marked 'S'. Unphysical domains for $K_d^{-1} \neq 0$, where condition (2.12) is violated, are marked 'unphys'.

The results of calculations are presented in figure 3. It is clear that even in the case of a very fast desorption (large but finite dimensionless desorption number K_d) the behaviour of the shortwave disturbances drastically changes. Even for $K_d = 10^3$ there is a strong damping of the shortwave oscillatory mode, and a competition between this mode and the longwave oscillatory mode takes place. Therefore, the interval of χ, where the shortwave mode is critical, diminishes in the presence of the sorption kinetics.

Note that this damping of the shortwave oscillatory mode is qualitatively similar to that found by Shklyaev & Nepomnyashchy (2011) for longwave mode at small L (quantitative agreement can be reached at as small L as 10^{-5} or less). The mechanism of the damping is the same for these two modes; the damping is caused by the advection of the surface phase (see the details in Shklyaev & Nepomnyashchy 2011).

Summarizing results on the linear stability analysis, we emphasize that the sorption kinetics leads to a very strong stabilization of the shortwave oscillatory mode, see

https://doi.org/10.1017/jfm.2012.619 Published online by Cambridge University Press

figure 3. Therefore, even rather fast kinetics makes this mode unimportant and only longwave modes can be critical. For both monotonic and oscillatory longwave modes the sorption leads to a well-pronounced stabilization as well, see figure 1.

4. Nonlinear dynamics of longwave disturbances

4.1. *Small K_{ad}: monotonic mode*

As we shall show below (see § 4.4), for finite K_{ad} the set of amplitude equations describing the evolution of longwave perturbations is ill-posed and a subcritical finite-amplitude excitation occurs. In contrast, for $K_{ad} = 0$ the adsorption kinetics is infinitely fast and the problem is reduced to that studied earlier (Oron & Nepomnyashchy 2004; Shklyaev *et al.* 2007), where supercritical excitation of the convection was found. (For the sake of convenience, we present the milestones of the cited papers in appendix A.) Thus, at sufficiently small values of the Langmuir number one can expect similar results. In the present subsection and in §§ 4.2 and 4.3, we perform a careful analysis of that case. The purpose is two-fold: first, for many surfactants the characteristic time of adsorption kinetics is small on the time scale of the convective motion. Second, this limiting case is interesting from the theoretical point of view, since the transition from the supercritical to the subcritical bifurcation can be thoroughly analysed.

In order to simplify the model, we restrict ourselves to the limiting case of fast desorption, i.e. $K_a = O(1)$, $K_d \gg 1$. In that case, neither K_a nor K_d separately, but only their ratio K_{ad}, appears in the governing equations. The small Langmuir number is retained only in (2.9); the surface concentration Γ has to be replaced with $C(z = 1)$ in the Marangoni stress and in the right-hand side of (2.9). (Throughout this subsection, §§ 4.2 and 4.3 we refer to the boundary conditions (2.6) keeping in mind all of these changes.) It should be noted that this assumption only shortens some expressions, qualitatively the analysis does not change considerably for finite K_d and small K_a.

To study the nonlinear dynamics of longwave disturbances, we rescale the coordinates and the time:

$$X = \epsilon x, \quad Y = \epsilon y, \quad \tau_2 = \epsilon^4 t, \tag{4.1}$$

and represent small K_{ad} and the Marangoni number as follows:

$$K_{ad} = \epsilon^2 k_{ad}, \quad k_{ad} = O(1), \tag{4.2}$$

$$M = 48(m_0 + \epsilon^2 m_2 + \cdots). \tag{4.3}$$

Here the small parameter ϵ is introduced via (3.3), so that the conventional asymptotics is considered. We start our analysis with the case $K_{ad} = O(\epsilon^2)$ which, as will be shown below, is a distinguished one in the sense that if $K_{ad} = o(\epsilon^2)$ the adsorption does not influence the leading order dynamics, while in the case $\epsilon^2 \ll K_{ad} \ll 1$ the structure of the amplitude equations is changed drastically (that case will be considered in § 4.3).

The fields of disturbances are sought in the form

$$\boldsymbol{u} = \epsilon \boldsymbol{U}, \quad w = \epsilon^2 W, \quad p = P, \tag{4.4a}$$

$$T = T_0(z) + \theta(\boldsymbol{R}, \tau_2) + \epsilon^2 \Theta(\boldsymbol{R}, z, \tau_2), \tag{4.4b}$$

$$C = \chi(z - 1) + \Gamma(\boldsymbol{R}, \tau_2) + \epsilon^2 \Sigma(\boldsymbol{R}, z, \tau_2), \tag{4.4c}$$

which is known to be appropriate in the absence of the surfactant adsorption on the surface (Oron & Nepomnyashchy 2004; Shklyaev *et al.* 2007). Hereafter $\boldsymbol{R} = (X, Y)$.

https://doi.org/10.1017/jfm.2012.619 Published online by Cambridge University Press

It should be noted that we explicitly extract the temperature in the base state T_0 from the temperature distribution, but include the constant Γ_0 into Γ. Therefore, instead of (2.12), the condition $3\min_z(\Gamma+\chi(z-1)) > \max_z(\Gamma+\chi(z-1))$ has to be valid for Γ at any X, Y and τ_2.

Next, we expand the disturbances

$$f = f^{(0)} + \epsilon^2 f^{(2)} + \cdots, \quad f = (\Theta, \Gamma, \Sigma, \boldsymbol{U}, W, P) \tag{4.5}$$

into series in ϵ^2. Substituting these expansions into (2.5) and (2.6), we collect the terms of zero and second order with respect to ϵ.

The concentration and temperature perturbations in the leading order are z-independent:

$$\theta = F(X, Y, \tau_2) + \theta_{00}(\tau_2), \quad \Gamma^{(0)} = G(X, Y, \tau_2). \tag{4.6}$$

Here we have separated out a part $\theta_{00}(\tau_2)$ from F in a way that will be explained below, see (4.9).

The velocity field in the zeroth order agrees with that found within the linear stability problem:

$$\boldsymbol{U}^{(0)} = 12m_0(2z-3z^2)\nabla h, \quad W^{(0)} = 12m_0(z^3-z^2)\nabla^2 h, \tag{4.7}$$

where $h = F + G$ is the surface tension perturbation up to the sign and an unimportant additive function of τ_2.

The solvability conditions in the zeroth order determine the stability boundary, given by $m_0 = m_*^{(m)}$ for $K_{ad} = 0$, see (A 1). In addition, these conditions determine a relation between $\nabla\theta$ and $\nabla\Gamma^{(0)}$. With an appropriate choice of $\theta_{00}(\tau_2)$, such that

$$\langle F\rangle = -\frac{\Gamma_0}{\chi(1+L^{-1})}, \tag{4.8}$$

we obtain that F and G are connected as follows:

$$F = -\frac{G}{\chi\left(1+L^{-1}\right)}. \tag{4.9}$$

Here the angle brackets denote a space-averaged value of the corresponding field and $\langle G\rangle = \Gamma_0 = N/(48m_0) + \chi/2$ with m_0 given by (A 1).

In the second order the calculations result in the following amplitude equation

$$\begin{aligned}\bar{\alpha}\dot{F} = {} & (1-\chi)(F-\langle F\rangle) + \bar{\gamma}_2\nabla^4 F + \nabla^2(\bar{\gamma}_1 F + \bar{\gamma}_4|\nabla F|^2 + \bar{\gamma}_7 F^2) \\ & + \bar{\gamma}_6 \boldsymbol{J}\cdot\nabla F + \nabla\cdot(\bar{\gamma}_3\nabla^2 F\nabla F - \bar{\gamma}_5|\nabla F|^2\nabla F),\end{aligned} \tag{4.10}$$

where the dot denotes a derivative with respect to τ_2, $\bar{\alpha} = \chi(1+L^{-1}+L^{-2}) - 1$ and $\bar{\gamma}_j$ ($j = 1$–7) are given in appendix B; $\boldsymbol{J} = \nabla\nabla^{-2}\nabla\cdot(\nabla^2 F\nabla F) - \nabla^2 F\nabla F$ is proportional to the toroidal component of the velocity.

For $k_{ad} = 0$ the coefficient $\bar{\gamma}_7$ vanishes and (4.10) coincides with (39) in Oron & Nepomnyashchy (2004); for non-zero k_{ad}, only $\bar{\gamma}_1$ is changed in addition to $\bar{\gamma}_7$. In particular, the coefficient $\tilde{\gamma}_5$ is the same as in the cited paper, being positive. It means that the cubic term itself corresponds to a supercritical bifurcation. With increase in k_{ad}, the quadratic term with the coefficient $\tilde{\gamma}_7$ becomes prevailing and (4.10) reduces to the Sivashinsky equation (Sivashinsky 1983), which is known to provide a subcritical bifurcation. (See also the remark concerning the Sivashinsky equation in § 4.4.) Thus, the amplitude equation describes the change of the direction of branching as k_{ad} grows.

https://doi.org/10.1017/jfm.2012.619 Published online by Cambridge University Press

This, in particular, means that for finite K_{ad} a subcritical excitation takes place, in accordance with the announced results at finite K_{ad}, see § 4.4.

Within this subsection we deal with the critical perturbations, which correspond to the minimum ($m_2 = m_{2c}$ at $K = K_c$) of the neutral stability curve $m_{2*}(K)$ determined by the relation

$$(1-\chi) - K^2(\bar\gamma_1 + 2\bar\gamma_7\langle F\rangle) + K^4\bar\gamma_2 = 0. \tag{4.11}$$

This leads to

$$\bar\gamma_0 m_{2c} = 2\sqrt{(1-\chi)\bar\gamma_2} - \frac{k_{ad}L_s\chi}{L^2}(1+L) - 2\bar\gamma_7\langle F\rangle, \quad K_c^4 = \frac{1-\chi}{\bar\gamma_2}, \tag{4.12}$$

where $\bar\gamma_0 = (1-\chi-\chi L^{-1})^2$. It is important for further analysis, that the critical value of m_2 has only a K-independent correction due to the adsorption kinetics and, therefore, the critical wavenumber K_c is not affected by k_{ad}, N and L_s.

First, we perform the weakly nonlinear analysis on a square lattice within (4.10). To that end F is represented in the following form:

$$\begin{aligned} F = \langle F\rangle &+ \delta(a\cos K_cX + b\cos K_cY) \\ &+ \delta^2[A_2(a^2\cos 2K_cX + b^2\cos 2K_cY) + B_2ab\cos K_cX\cos K_cY] + \cdots, \end{aligned} \tag{4.13}$$

$$A_2 = -\frac{K_c^2[K_c^2(\bar\gamma_3+2\bar\gamma_4)-2\bar\gamma_7]}{9(1-\chi)}, \quad B_2 = -\frac{2K_c^2(\bar\gamma_3K_c^2-2\bar\gamma_7)}{1-\chi}. \tag{4.14}$$

It should be emphasized that the steady patterns on a square lattice can be observed in a confined layer of a square horizontal cross-section with adiabatic and impermeable for both phases of the surfactant vertical walls. Indeed, the boundary conditions $\nabla_n F = \nabla_n h = 0$ at the sidewalls ensure zero normal velocity at the boundary, whereas the no-slip conditions are satisfied in a thin (on the typical longitudinal scale) layer near the boundaries. Hence, the periodical patterns studied below can be also experimentally found in the domain of the horizontal length π/K (or $n\pi/K$ with any natural integer n).

The amplitudes a and b satisfy the set of two algebraic equations

$$\bar\gamma_0(m_2 - m_{2c})a = (K_0a^2 + K_1b^2)a, \tag{4.15a}$$

$$\bar\gamma_0(m_2 - m_{2c})b = (K_0b^2 + K_1a^2)b, \tag{4.15b}$$

where

$$K_0 = [\tfrac{3}{4}\bar\gamma_5 - A_2(\bar\gamma_3+2\bar\gamma_4)]K_c^2 - A_2\bar\gamma_7, \tag{4.16}$$

$$K_1 = [\tfrac{1}{2}\bar\gamma_5 + B_2(\bar\gamma_3-\bar\gamma_4)]K_c^2 - B_2\bar\gamma_7. \tag{4.17}$$

It is readily seen that the Landau constants do not depend on L_s and N; therefore, the only parameter that characterizes an influence of the sorption kinetics on pattern selection is k_{ad}.

It is well known (Golubitsky, Swift & Knobloch 1984; Hoyle 2006) that rolls emerge through the direct bifurcation at

$$K_0 > 0, \tag{4.18}$$

whereas for squares supercritical branching takes place at

$$K_0 + K_1 > 0. \tag{4.19}$$

https://doi.org/10.1017/jfm.2012.619 Published online by Cambridge University Press

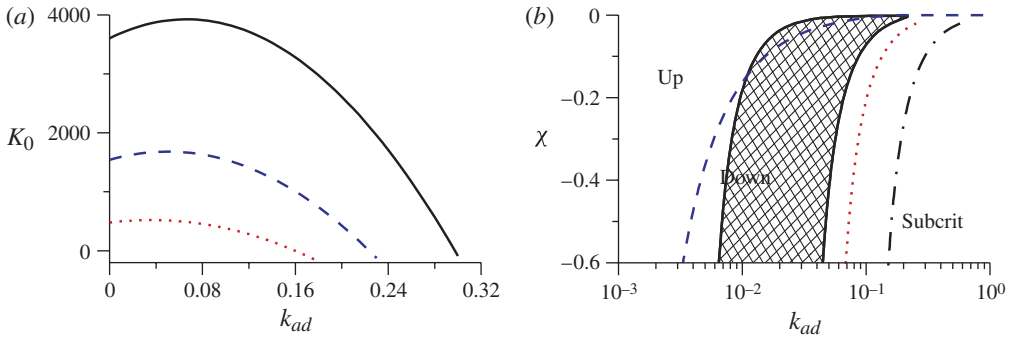


FIGURE 4. (Colour online) Pattern selection within (4.10) for $P = 2, L = 0.01$. (*a*) Variation of the Landau constants K_0, given by (4.16), with k_{ad}; the solid, dashed and dotted lines correspond to $\chi = -0.1, -0.2$ and -0.5, respectively. (*b*) Pattern selection on square and hexagonal lattices; the dot-dashed (dotted) line separates domains of supercritical and subcritical bifurcations for rolls (squares) (subcritical bifurcations take place to the right of the curves); rolls are selected on a square lattice within the crosshatched area, squares are selected beyond this area and to the left of the dotted line. The dashed line corresponds to $Q = 0$ for hexagons (4.22); this line separates up and down hexagons; near this line (4.23) is valid.

Under conditions (4.18) and (4.19), rolls are selected on a square lattice at $K_1 > K_0$, otherwise squares are selected.

The self-interaction coefficient, K_0, is positive at $k_{ad} = 0$ and it becomes negative with increase in k_{ad}, as shown in figure 4(*a*). The cross-interaction coefficient, K_1, varies with k_{ad} in a qualitatively similar way, being less than K_0 almost everywhere.

The stability map in the plane $(k_{ad} - \chi)$ is presented in figure 4(*b*). It is clear that at small k_{ad} both patterns are supercritical and squares are selected. It is noteworthy that at larger k_{ad} a small area appears where rolls are selected. With increase in k_{ad}, the direction of branching changes for both squares and rolls. Thus, (4.15) describes the transition from squares selected for infinitely fast kinetics ($k_{ad} = 0$) (Oron & Nepomnyashchy 2004) to the subcritical bifurcation at $k_{ad} \gg 1$. Of course, subcritical branching within (4.10) does not lead to an infinite growth of the solution, since at large $|F(X, Y)|$ the stabilizing cubic term dominates. However, at the stable upper branch $F \sim k_{ad}$ at large k_{ad}.

In fact, it is well known (see Golubitsky *et al.* 1984; Hoyle 2006) that quadratic terms in the amplitude equation (4.10) lead to a subcritical excitation of hexagons due to resonant interaction of rolls with the wavevectors $\boldsymbol{K}_1 = K_c(1, 0), \boldsymbol{K}_{2,3} = K_c(-1, \pm\sqrt{3})/2$. Therefore, all of the remaining patterns are unstable in infinite domains near the stability threshold unless the coefficient of quadratic interaction vanishes. (For the above-mentioned square pattern in a confined cavity of square horizontal cross-section the emergence of hexagons is prohibited owing to the boundary conditions.)

Thus, we address the branching of the hexagons, representing the solution in the form

$$F = \langle F \rangle + \delta\,(a \cos K_c X + b \cos \boldsymbol{K}_2 \cdot \boldsymbol{R} + c \cos \boldsymbol{K}_3 \cdot \boldsymbol{R}) + \cdots. \tag{4.20}$$

The stationary solution for the hexagons is governed by the equation

$$\bar{\gamma}_0(m_2 - m_{2c})a + Qbc = 0, \tag{4.21}$$

https://doi.org/10.1017/jfm.2012.619 Published online by Cambridge University Press

and a pair of equations produced from (4.21) by a cyclic permutation of the amplitudes a, b and c. Here Q is given by

$$Q = -\frac{\bar{\alpha}}{2} - \frac{1}{10P}(1 - \chi - \chi L^{-1}) + \frac{12\chi}{LK_c^2}(1 + L^{-1})k_{ad}. \tag{4.22}$$

When this coefficient is positive, up hexagons are selected (liquid rises in the middle of a cell), in the opposite case down hexagons emerge. For the infinitely fast kinetics, when the last term in (4.22) is zero, the selected pattern is determined by the Prandtl number, χ and L as was found by Oron & Nepomnyashchy (2004). An example of calculations is presented in figure 4(*b*). For heating from below ($m_0 > 0$, $\chi < 0$), with increase in k_{ad}, down hexagons are selected. The opposite situation takes place for heating from above ($m_0 < 0$, $\chi > \chi_1 > 0$), when up hexagons are selected at large k_{ad}.

Near the locus of $Q = 0$, the cubic nonlinear terms become comparable with the quadratic one, and the amplitudes are defined by the following equation

$$\bar{\gamma}_0(m_2 - m_{2c})a + Q_1 bc = K_0 a^3 + K_2(b^2 + c^2)a, \tag{4.23}$$

and a similar pair of equations for b and c. Here $Q_1 = Q/\delta$. The cubic terms are stabilizing along the curve $Q = 0$ (see figure 4*b* for K_0), therefore in the case of small, but non-zero Q, a saddle-node bifurcation takes place at a certain $m_2 < m_{2c}$, which leads to emergence of a stable branch of hexagons. Numerical calculations show that $K_2 > K_0$ along the dashed line in figure 4(*b*), i.e. with increase in m_2 this branch of hexagons loses the stability and at larger m_2 rolls are selected on a hexagonal lattice (Golubitsky *et al.* 1984; Golovin, Nepomnyashchy & Pismen 1995; Hoyle 2006). The condition, which determines a stability of squares with respect to hexagons (Golovin *et al.* 1995), is also valid along the dashed line. Therefore, with increase in m_2 the stable pattern is selected by the stability analysis within (4.15): except for the small cross-hatched area in figure 4(*b*), squares are selected in this case.

4.2. *Small K_{ad}: oscillatory mode, case I*

We now proceed to the analysis of the oscillatory mode in the same limiting case, $K_{ad} \ll 1$, again dealing with the limit of fast desorption ($K_d \gg 1$, $K_a = O(1)$).

Substituting expansions given by (3.3) and (4.1)–(4.5) supplemented with an additional time scale $\tau = \epsilon^2 t$ into (2.5) and (2.6) one can repeat the procedure similar to that carried out by Shklyaev *et al.* (2007). We do not present all of the details, referring instead to the cited paper and giving a brief summary of the results in appendix A.

In the zeroth order the velocity components are given by (4.7) with $h = F + \tilde{G}$. Here we introduce F and G according to (4.6) with $\theta_{00} = \langle\theta\rangle$ and set $G = \Gamma_0 + \tilde{G}$, assuming that mean values of F and $\tilde{G}$ are zero. (Again, $\Gamma_0 = N/(48m_0) + \chi/2$, but m_0 is now defined by (A 2).)

In the second order we arrive at the linear amplitude equations:

$$L_1(F, G) = L_2(F, G) = 0, \tag{4.24}$$

where

$$L_1 = F_\tau - \nabla^2[(1 - m_0)F - m_0 G], \tag{4.25}$$

$$L_2 = G_\tau - \nabla^2[\chi(L + m_0)F + (L + \chi m_0)G]. \tag{4.26}$$

Here, as we have stated above, m_0 is given by (A 2) and, therefore, the solution oscillates in τ with the frequency Ω, see (A 3).

https://doi.org/10.1017/jfm.2012.619 Published online by Cambridge University Press

Proceeding to the fourth order and demanding the solvability of the corresponding boundary-value problem, we arrive at (A 5) and (A 6) with additional term $k_{ad}\sigma_n$,

$$\sigma_n = G_\tau - 12m_0\nabla\cdot(G\nabla h) - L_s\nabla^2 G, \tag{4.27}$$

in the right-hand side of (A 6). (The derivative G_τ has to be replaced with terms proportional to $\nabla^2 F$ and $\nabla^2 G$ via (4.24).)

In order to describe the nonlinear dynamics within this approach, one has to write a general solution of (4.24) as a superposition of travelling waves, which possesses a certain symmetry. (The Fourier amplitudes depending on τ_2 can be arbitrary at this stage.) Then it is necessary to demand the solvability of non-homogeneous linear problem (A 5) and (A 6) with the above-mentioned correction. Its solvability conditions serve as evolutionary equations for the Fourier amplitudes.

The new term which stems from the adsorption kinetics, $k_{ad}\sigma_n$, includes both linear and quadratic contributions. The linear contribution results in a correction to the growth rate, proportional to $k_{ad}K^2$:

$$\gamma = \gamma^{(o)} - \frac{k_{ad}K^2}{2}\left[1 + L_s + \frac{N}{4} - m_0(1-6\chi)\right] - \frac{\mathrm{i}k_{ad}K^2}{2\Omega}\left[L_s + \frac{N}{4} - \Omega^2 - m_0(L_s - 6\chi)\right], \tag{4.28}$$

where $\gamma^{(o)}$ is given by (A 11).

The adsorption-induced term in γ can be calculated via (3.11) at small K_{ad}. It is important that this term is proportional to K^2 similarly to the term containing m_2. In particular, this means that the critical value of m_2 has only a K-independent correction due to the adsorption kinetics and, again, the critical wavenumber K_c is independent of k_{ad}, N and L_s. Similarly to § 4.1, below we fix $K = K_c$ and $m_2 = m_{2c}$, corresponding to the minimum of the neutral stability curve $m_2(K)$ for the oscillatory mode.

Quadratic nonlinearity influences only pattern selection on a square lattice (Pismen 1988; Shklyaev *et al.* 2007), whereas branching for rolls, rhombic patterns (Shklyaev *et al.* 2007) and hexagons (Shklyaev *et al.* 2009*a*, 2011) remains unchanged. All patterns on these lattices bifurcate supercritically.

Let us briefly discuss the results for a square lattice, representing the solution of (4.24) in the following form:

$$h = \delta(A_1\mathrm{e}^{\mathrm{i}K_cX} + A_2\mathrm{e}^{-\mathrm{i}K_cX} + B_1\mathrm{e}^{\mathrm{i}K_cY} + B_2\mathrm{e}^{-\mathrm{i}K_cY})\mathrm{e}^{-\mathrm{i}\Omega K_c^2\tau} + \delta^2(C_1\mathrm{e}^{\mathrm{i}\phi_+} + C_2\mathrm{e}^{-\mathrm{i}\phi_+} + C_3\mathrm{e}^{-\mathrm{i}\phi_-} + C_4\mathrm{e}^{\mathrm{i}\phi_-})\mathrm{e}^{-2\mathrm{i}\Omega K_c^2\tau} + \mathrm{c.c.} + \cdots \tag{4.29}$$

$$\phi_+ = K_c(X+Y), \quad \phi_- = K_c(X-Y). \tag{4.30}$$

Here the small factor δ^2 is a measure of the supercriticality $m_2 - m_{2c}$; A_j and B_j $(j = 1, 2)$ are the complex amplitudes of four base travelling waves, whereas C_j $(j = 1$–$4)$ are the amplitudes of four oblique waves. These oblique waves are generated through the quadratic interaction of the type $A_1 \times B_1 \to C_1$, etc., and, in turn, they influence the nonlinear growth of the base waves via the quadratic interactions $C_1 \times B_1^* \to A_1$ and $C_4 \times B_2^* \to A_1$ (the asterisk denotes the complex conjugation). This leads to a conventional set of the amplitude equations governing a pattern selection on a square lattice (Silber & Knobloch 1991):

$$\dot{A}_1 = [\gamma_2 - K_0|A_1|^2 - 2K_1|A_2|^2 - K_2(|B_1|^2 + |B_2|^2)]A_1 - K_3A_2^*B_1B_2, \tag{4.31a}$$

$$\dot{A}_2 = [\gamma_2 - K_0|A_2|^2 - 2K_1|A_1|^2 - K_2(|B_1|^2 + |B_2|^2)]A_2 - K_3A_1^*B_1B_2, \tag{4.31b}$$

https://doi.org/10.1017/jfm.2012.619 Published online by Cambridge University Press

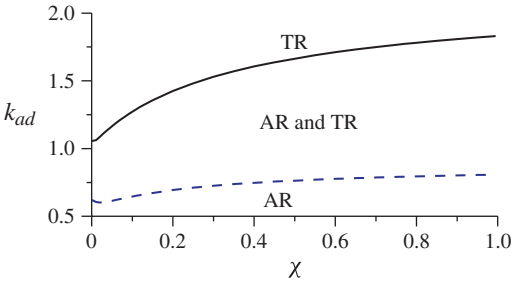


FIGURE 5. (Colour online) Pattern selection on a square lattice within (4.31); $P = 2$, $L = 0.01$. Domains of stability for alternating rolls and travelling rolls are marked 'AR' and 'TR', respectively. In the domain marked 'AR and TR', multistability occurs.

and a pair of similar equations for $B_{1,2}$. Here the dot denotes the time derivative, which are small, $O(\delta^2)$, and

$$\gamma_2 = \frac{\partial \gamma}{\partial m_2}(m_2 - m_{2c}). \tag{4.32}$$

Recall that Silber & Knobloch (1991) found five limit cycles within (4.31). Two of them, travelling rolls (TRs) and standing rolls (SRs), are one dimensional, whereas the remaining three, travelling squares (TSs), standing squares (StSs) and alternating rolls (ARs) are genuine square patterns. (Under certain conditions there also exist standing cross rolls, but they are always unstable.)

For the infinitely fast kinetics the coefficients of the nonlinear interactions are given by (A 14). The above-mentioned adsorption-induced term in (A 6) replaces only $\mu^{(o)}$ and $\mu_2^{(o)}$, given by (A 14*d*), with μ and μ_2, respectively:

$$\mu = \mu^{(o)} + \frac{6m_0K_c^2k_{ad}}{1+\Omega^2}\left\{1 - 2m_0 + \Omega^2 + \frac{\mathrm{i}}{\Omega}[1 + \Omega^2 + m_0(\Omega^2 - 1)]\right\}, \tag{4.33a}$$

$$\mu_2 = \mu_2^{(o)} + 12m_0K_c^2k_{ad}\left[1 + \frac{\mathrm{i}}{\Omega}(1 - m_0)\right]. \tag{4.33b}$$

The change in the growth rate γ does not influence the denominator in K_2, see (A 14*b*). Indeed, new terms included in (4.28) are proportional to K^2 and therefore $\gamma_0(\sqrt{2}K_c) - 2\gamma_0(K_c) = \gamma_0^{(o)}(\sqrt{2}K_c) - 2\gamma_0^{(o)}(K_c)$. Thus, the replacement of μ and μ_2 according to (4.33) is the only consequence of the adsorption kinetics. As has been emphasized above, K_c is independent of the k_{ad}. This, in particular, means that all of the nonlinear coefficients remain fixed under variation of both N and L_s.

The calculations show that all five patterns found by Silber & Knobloch (1991) bifurcate supercritically (Shklyaev *et al.* 2007). Of course, for one-dimensional patterns there is no oblique waves at all and, hence, the directions of branching for TR and SR do not depend on k_{ad}. However, stability of these patterns is determined by the rescaled Langmuir number.

Pattern selection studied within (4.31) indicates that with the increase in k_{ad} ARs lose their stability, whereas TRs become stable. It is clear from figure 5, that there is an interval of k_{ad}, where both above-mentioned patterns are stable.

The selection of wavy patterns in a confined cavity is, generally speaking, a complicated task. However, for the particular case discussed in § 4.1, a domain of

https://doi.org/10.1017/jfm.2012.619 Published online by Cambridge University Press

a square horizontal cross-section with adiabatic boundaries ($\nabla_n F = \nabla_n \Gamma = 0$), the answer is simple. This boundary condition corresponds to reflection of the waves and, hence, it supports standing waves, but suppresses the travelling waves. Therefore, ARs, which is a superposition of two standing waves, survive. Only the spectrum of wavenumbers (and, hence, frequencies) becomes discrete: the horizontal cavity length should be equal to an integer number of half-wavelengths. In contrast, TRs cannot be found in this case unless the cavity length is large in comparison with a wavelength of TRs.

4.3. *Small K_{ad}: oscillatory mode, case II*

As we have shown in §§ 4.1 and 4.2, in the case $K_{ad} = O(\epsilon^2)$ the amplitude equations are similar to those with $K_{ad} = 0$, except for the appearance of additional terms. The structure of the amplitude equations changes drastically with the growth of K_{ad}. As the next step, let us consider the case

$$K_{ad} = \epsilon \tilde{k}_{ad}, \tag{4.34}$$

which is relevant for the oscillatory mode. (Again K_d is assumed large.) According to the results of § 4.2, only the one-dimensional solution has to be considered, because for large k_{ad} (but small $\tilde{k}_{ad}$) TR is the only stable pattern.

Then, we introduce the first slow time $\tau_1 = \epsilon^3 t$, and add terms of odd orders in ϵ to expansions given by (4.3)–(4.5):

$$f = f^{(0)} + \epsilon f^{(1)} + \cdots, \quad f = (\theta, \Theta, \Gamma, \Sigma, \boldsymbol{U}, W, P), \tag{4.35}$$

$$m = m_0 + \epsilon m_1 + \cdots. \tag{4.36}$$

Repeating all of the calculations one can see that the problems in the zeroth and second orders do not change, whereas the solution in the first order reads:

$$\theta^{(1)} = F_1(X, Y, \tau_2), \quad \Gamma^{(1)} = G_1(X, Y, \tau_2), \quad h_1 = F_1 + G_1, \tag{4.37}$$

$$\boldsymbol{U}^{(1)} = 12(2z - 3z^2)\boldsymbol{\nabla}(m_0 h_1 + m_1 h), \tag{4.38}$$

$$W^{(1)} = 12(z^3 - z^2)\nabla^2(m_0 h_1 + m_1 h). \tag{4.39}$$

This solution is an obvious extension of (4.6) and (4.7) to the first order.

The one-dimensional solution of (4.24), the solvability conditions in the second order, is

$$h = \delta(A_1 \mathrm{e}^{\mathrm{i}KX} + A_2 \mathrm{e}^{-\mathrm{i}KX})\mathrm{e}^{-\mathrm{i}\Omega K^2 \tau} + \text{c.c.}, \tag{4.40}$$

where the complex amplitudes of two counter-propagating waves depend on the slow times τ_1, τ_2, etc.

The solvability conditions in the third-order are:

$$L_1(F_1, G_1) = -m_1 h_{XX} - \partial_{\tau_1} F, \tag{4.41}$$

$$L_2(F_1, G_1) = \chi m_1 h_{XX} - \partial_{\tau_1} G - \tilde{k}_{ad} \tilde{\sigma}_n, \tag{4.42}$$

where $\tilde{\sigma}_n$ is the one-dimensional reduction of (4.27). We split $\tilde{\sigma}_n$ into two parts, $\tilde{\sigma}_{nl}$, linear with respect to F and G, and $\tilde{\sigma}_{nn}$, quadratic in F and G, as follows

$$\tilde{\sigma}_{nl} = G_\tau - 12 m_0 \Gamma_0 h_{XX} - L_s G_{XX}, \tag{4.43}$$

$$\tilde{\sigma}_{nn} = -12 m_0 (\tilde{G} h_X)_X, \quad \tilde{G} = G - \Gamma_0, \quad \Gamma_0 = \frac{N}{48 m_0} + \frac{\chi}{2}. \tag{4.44}$$

https://doi.org/10.1017/jfm.2012.619 Published online by Cambridge University Press

Only $\tilde{\sigma}_{nl}$ contributes into the solvability condition of the linear set of (4.41) and (4.42), whereas $\tilde{\sigma}_{nn}$ does not produce any resonant terms within the one-dimensional problem. Dealing with the neutrally stable solution, we set $(\tilde{G}, F) \sim \exp(-\mathrm{i}\Omega_1 K^2 \tau_1)$ and find out the correction to the Marangoni number,

$$m_1 = \tilde{k}_{ad} \frac{1 + L_s + N/4 - m_0(1 - 6\chi)}{1 - \chi}, \tag{4.45}$$

and to the frequency, Ω_1. Both of these quantities can be extracted from (3.16) and (3.17) at small values of the Langmuir number. A particular solution of (4.41) and (4.42), linear with respect to F and G, is unimportant for the further analysis, whereas the nonlinear part of the solution is

$$h_n^{(1)} = -\frac{4m_0\tilde{k}_{ad}}{\Omega^2}[\xi(A_1^2 \mathrm{e}^{2\mathrm{i}KX} + A_2^2 \mathrm{e}^{-2\mathrm{i}KX})\mathrm{e}^{-2\mathrm{i}\Omega\tau} + 3(\xi_r - 1 + m_0)A_1 A_2^* \mathrm{e}^{2\mathrm{i}KX}] + \mathrm{c.c.}, \tag{4.46}$$

where $\xi = \xi_r + \mathrm{i}\xi_i = (1 - m_0 + \mathrm{i}\Omega)(2 + \mathrm{i}\Omega)/(1 + \mathrm{i}\Omega)$. The corresponding part of the surface concentration $\Gamma_n^{(1)}$ can be easily expressed using $h_n^{(1)}$.

In the fourth order we obtain the one-dimensional reduction of (A 5) and (A 6) with the additional term $12m_0\tilde{k}_{ad}\,(\Gamma_n^{(1)}h_X + \tilde{G}h_{nX}^{(1)})_X$ in the right-hand side of (A 6). There are also a number of linear and quadratic terms which do not directly influence the weakly nonlinear behaviour of TRs. Moreover, the contribution of the linear terms to the growth rate is of the form $\tilde{k}_{ad}^2 K^2$; therefore, similarly to case I m_2 has only a K-independent correction due to the adsorption kinetics and the critical wavenumber remains the same as for $K_{ad} = 0$ (Oron & Nepomnyashchy 2004).

The solvability conditions yield the following set of amplitude equations:

$$\dot{A}_1 = (\gamma_2 - K_0\,|A_1|^2 - K_1\,|A_2|^2)A_1, \tag{4.47a}$$

$$\dot{A}_2 = (\gamma_2 - K_0\,|A_2|^2 - K_1\,|A_1|^2)A_2. \tag{4.47b}$$

The real parts of the self- and cross-interaction coefficients are given by

$$K_{0r} = \alpha_r^{(o)} - \frac{72m_0^2\tilde{k}_{ad}^2K^2}{\Omega^2(1 + \Omega^2)}[(2m_0 - 1)(m_0 - 1) + \Omega^2(1 + m_0)], \tag{4.48a}$$

$$K_{1r} = 2\alpha_r^{(o)} + \frac{72m_0^2\tilde{k}_{ad}^2K^2}{\Omega^2(1 + \Omega^2)}(m_0 + 1)(L + L^2), \tag{4.48b}$$

where $\alpha^{(o)}$ is given by (A 14*c*) and the subscript r refers to the real part of a corresponding coefficient. It is clear that the contribution of the sorption kinetics into K_{0r} is negative, i.e. K_{0r} becomes negative for rather large $\tilde{k}_{ad}$. At $K_{ad} = O(\epsilon^2)$ (small $\tilde{k}_{ad}$) the last term in K_0 vanishes and the formula $K_{0r} = \alpha_r^{(o)}$ is restored, see § 4.2.

The domain of supercritical Hopf bifurcation in the plane $(\chi - \tilde{k}_{ad})$ is shown in figure 6. Plotting this figure we again consider critical perturbations thus setting $K = K_c$. It is worth noting, that both L_s and N contribute to $K_{0,1}$ neither directly nor by means of the selection of the critical wavenumber K_c. Therefore, the presented plot is valid irrespectively of these two parameters.

It is also noteworthy that the same approach for the pattern selection on a hexagonal lattice leads to changes in all constants of nonlinear interaction similar to that for rolls, cf. (4.48). This, generally speaking, breaks the degeneracy found by Shklyaev

https://doi.org/10.1017/jfm.2012.619 Published online by Cambridge University Press

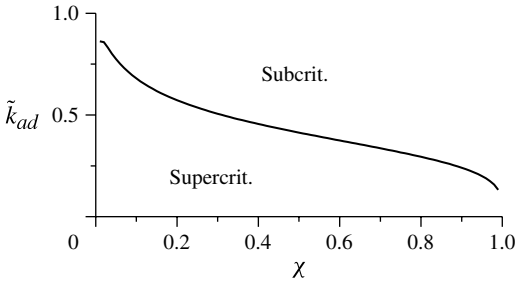


FIGURE 6. Direction of branching for the wavy patterns, case II. Domains of supercritical and subcritical bifurcations for TRs within (4.47) and (4.48); $P = 2,\ L = 0.01$.

et al. (2009*a*, 2011). The pattern selection for this case can be carried out on the base of Roberts, Swift & Wagner (1986), although such analysis lies beyond the scope of this paper.

4.4. *Nonlinear evolution at finite K_{ad}*

We now proceed to the finite values of the Langmuir number, applying the expansions (3.3), (4.1), (4.4) and (4.5). The Marangoni number is not expanded in ϵ, but it is rescaled according to the relation $M = 48m$.

The solvability conditions in the leading order of expansion read

$$\theta_\tau = \nabla^2(\theta - mh), \tag{4.49a}$$

$$\Gamma^{(0)}_\tau = \nabla^2 \frac{(L + K_{ad}L_s)\Gamma^{(0)} + L\chi\theta + m\chi h}{1 + K_{ad}} + \frac{12mK_{ad}}{1 + K_{ad}} \boldsymbol{\nabla} \cdot (\Gamma^{(0)} \boldsymbol{\nabla} h). \tag{4.49b}$$

Linearization of (4.49) around $\Gamma^{(0)} = \Gamma_0$ and $\theta = 0$ provides the linear stability problem studied in § 3.1. In the limit $K_{ad} \gg 1$, $\chi = 0$ (4.49) reduces to (151) and (152) of Mikishev & Nepomnyashchy (2010*b*) valid for an insoluble surfactant. It is also worth noting that a similar set of amplitude equations was analysed by Goldobin & Lyubimov (2007) for axisymmetric regimes with a source of solute at the origin. Both distinctions, the axial symmetry and the presence of the source, are crucial and therefore the results obtained by Goldobin & Lyubimov (2007) cannot be used for the problem under consideration.

It should be emphasized that there is a crucial difference between the leading-order amplitude equation (4.10), and those obtained in the absence of adsorption by Oron & Nepomnyashchy (2004) or for small K_{ad}, see (4.24). Indeed, in the latter case, in the framework of the Boussinesq approximation, the evolution of perturbation in τ is governed by the gradient of the temperature and concentration perturbations rather than by these perturbations themselves. Hence, the nonlinear terms in the amplitude equations contain additional differentiations with respect to spatial variables, thus they have a higher smallness order in the longwave limit than the nonlinear term in (4.49*b*).

In the case $K_{ad} = 0$ (or $K_{ad} = O(\epsilon)$, see §§ 4.1–4.3), (4.49) are linear and they determine the critical value of $m = m_*$ where the longwave finite-amplitude disturbances of the temperature and concentration neither grow nor decay. In the case of finite Langmuir number, $K_{ad} = O(1)$, there is no such value of m at all. Indeed, the full nonlinear set of equations describes coupled nonlinear diffusion of two scalar fields with the 'diffusivities' depending on $\Gamma^{(0)}$. It is obvious, that above the stability threshold, given by (3.14) or (3.16), an effective diffusivity becomes negative. In this

https://doi.org/10.1017/jfm.2012.619 Published online by Cambridge University Press

case the problem is ill-posed and the system evolution results in an infinitely fast growth of short waves. This leads to the growth of shortwave perturbations (or at least perturbations with a characteristic length scale smaller than ϵ^{-1}) over the entire layer. The set of amplitude equations cannot be regularized by addition of a certain stabilizing term in this case, except for the situations discussed in the last paragraph of this subsection. One of the possible hypotheses of the further dynamics of the system is that the finite-amplitude shortwave convection sets in.

Moreover, it can be readily shown in the one-dimensional case that both monotonic and oscillatory spatially periodic solutions bifurcate subcritically within (4.49). Thus, for finite-amplitude perturbations, the problem is ill-posed even below the stability threshold.

For the steady state, when $\Gamma^{(0)} = \Gamma_0 + \Gamma_s = N/(48m) + \chi/2 + \Gamma_s$ and $\theta_s = mh_s = m\Gamma_s/(1-m)$, equation (4.49) reduces to

$$\nabla \cdot [D_{eff}(\Gamma_s)\nabla\Gamma_s] = 0, \tag{4.50}$$

where

$$D_{eff} = \frac{1}{(1-m)(1+K_{ad})}\left[\frac{m_*^{(m)} - m}{m_*^{(m)}}\left(L + K_{ad}\left(L_s + \frac{N}{4}\right)\right) + 12K_{ad}m\Gamma_s\right]. \tag{4.51}$$

The latter quantity vanishes at

$$\Gamma_s = \Gamma_c = -\left(1 - \frac{m}{m_*^{(m)}}\right)\frac{L + K_{ad}(L_s + N/4)}{12mK_{ad}}, \tag{4.52}$$

which can be treated as a lower boundary of a basin of attraction for the base state. The initial perturbation, which does not violate the condition $\Gamma^{(0)}(\boldsymbol{R}, \tau = 0) > \Gamma_0 + \Gamma_c$ for any X and Y, decays and the surface concentration approaches its mean value Γ_0.

Let us discuss the expected evolution in the simplest two-dimensional system when the initial profile of the surface concentration $\Gamma(X, \tau = 0)$ has one maximum (at $X = 0$) and one minimum (at $X = L$) over the domain $0 < X < L$; the minimum value of $\Gamma(\tau = 0)$ is slightly less than $\Gamma_0 + \Gamma_c$. (Such a system can be thought of as a half of a spatially periodic solution or a system confined by rigid walls at $X = 0, L$.) We expect a subcritical excitation of the shortwave convection near $X = L$ whereas the longwave convection in the remaining domain transports the surfactant towards the point $X = 0$. The advection of the surfactant results in a sharp peak in Γ around the point $X = 0$ and triggers a shortwave flow as well. Therefore, a couple of fronts separating domains of shortwave and longwave convection appears. The dynamics of these fronts can be described by a matching procedure, but numerical computations are needed to calculate the finite-amplitude shortwave convection (unlike the case considered by Bernoff (1988)). Such an analysis lies beyond the scope of the current paper.

The well-posedness of the system of amplitude equations can be restored only by taking into account the quartic terms in the linear dispersion relation, i.e. by adding the terms with fourth derivatives. This procedure was materialized in §§ 4.1–4.3 for sufficiently fast sorption kinetics. Another example can be provided by revisiting the scaling (4.4) assuming both θ and $\tilde{\Gamma}$ to be $O(\epsilon^2)$. However, such an analysis for the monotonic mode results in the Sivashinsky equation (Sivashinsky 1983), which is known to be ill-posed as well (Bernoff & Bertozzi 1995; Nepomnyashchy *et al.* 2004). Thus, we come to the conclusion that a longwave weakly nonlinear analysis based on the scaling determined by (4.1) and (4.4), is not self-consistent in the general case $K_{ad} = O(1)$.

https://doi.org/10.1017/jfm.2012.619 Published online by Cambridge University Press

5. Conclusions

We consider thermosolutocapillary convection in a heated thin film of a binary mixture. The solute is a surfactant, which is present in both surface and bulk phases.

Linear stability analysis clearly demonstrates the strong stabilization of the base conductive state in the presence of the adsorption/desorption kinetics. This stabilization takes place for the longwave monotonic and oscillatory modes (figure 1) and for the shortwave oscillatory mode (figure 3). It is known that usually (Palmer & Berg 1972; Nepomnyashchy & Simanovskii 1986; Ryabitskii 1993), in spite of strong damping of the monotonic mode in presence of surfactant, there is almost no stabilization of the layer, because of emerging oscillatory mode. In contrast, in our case the shortwave oscillatory mode is suppressed even more efficiently than the monotonic one. As shown in figure 3, this mode almost disappears in the presence of the sorption kinetics and advection of the surfactant over the free surface. It should be noted that in this paper we do not consider the transient growth effects due to the non-normality of the linearized evolution operator that are non-trivial in some cases, e.g. for open flows, see Blackburn, Sherwin & Barkley (2008) and references therein.

Weakly nonlinear analysis of longwave perturbations is carried out in the case of the small Langmuir number K_{ad}, which is the dimensionless ratio of the adsorption and desorption rates. The study performed at $K_{ad} \ll 1$ demonstrates the transition from a regular supercritical convective motion to a blowing up as K_{ad} increases. More precisely, the system is governed by the ratio of two asymptotic parameters $k_{ad} = K_{ad}/\sqrt{B}$, where B is the (small) Biot number. (In the case studied in § 4.3, $\tilde{k}_{ad} = K_{ad}/B^{1/4}$ is relevant.)

For steady convection, the competition of squares, rolls and hexagons is found. As shown in figure 4, either of these patterns can be stable under certain conditions. The selection of rolls is a remarkable feature of the sorption kinetics; at small values of the Biot number, stable rolls found neither for pure nor for binary liquid. With increase in k_{ad}, the branching changes its direction and subcritical bifurcation sets in.

Even more intricate variation with increase in K_{ad} takes place for the longwave oscillatory convection. Starting with stable alternating rolls (ARs) at $k_{ad} = 0$, we observe multistability region within a certain band of k_{ad} (see figure 5), where both ARs and travelling rolls (TRs) are stable and any of these two patterns can be reached depending on the initial conditions. Further growth of k_{ad} makes TR the only stable solution, which at finite $\tilde{k}_{ad}$ (or, equivalently, $k_{ad} \gg 1$, $K_{ad} \ll 1$) bifurcates subcritically, i.e. no stable patterns exist.

We also generalize the weakly nonlinear study to finite values of the Langmuir number. The set of amplitude equations for the general case is shown to be ill-posed: depending on the initial conditions, a perturbation either decays or blows up with fast growth of the short-scale perturbations. The mechanism of the blowing up is an advection of the surfactant along the free surface and this unbounded growth of perturbations is connected with the growth of the linear stability threshold as K_{ad} increases. It is more easy to explain that effect in the limit when the dimensionless desorption rate K_d is small, hence the surfactant is weakly soluble. The convective flow at the surface sweeps the surfactant and cleans the surface, except for the borders between the convective cells, where the divergence of the surface velocity is negative and the surfactant is collected. Hence, the threshold for the pure surface is effectively restored, which means the subcritical development of the instability. Of course, the blowing up ensues from the strong nonlinearity of the longwave approximation and its relatively weak dissipation, which cannot persist against the formation of the

https://doi.org/10.1017/jfm.2012.619 Published online by Cambridge University Press

large gradient of the surface concentration at the borders of the convective cells. 'shock waves' emerging can be resolved within direct numerical simulations of the full (unrescaled) convective problem.

For the calculations we choose the parameters typical for experiments (e.g. small Biot and Lewis numbers). Computations are performed in a wide range of the Soret number χ and dimensionless adsorption rate K_{ad}, covering most experimentally attainable situations. Changing the bulk concentration of the surfactant (and, hence, both χ and K_{ad}), one can track most the regimes described as well as the reported bifurcations between these patterns.

Our work is a natural extension of the previous papers on the longwave convection of binary liquid, the problem which provides a rare example of a longwave oscillatory mode. Allowing for the substantial progress in analytical solution, this problem is rather rich in possible scenarios and bifurcations (Pismen 1988; Clune, Depassier & Knobloch 1996; Oron & Nepomnyashchy 2004; Shklyaev *et al.* 2007, 2009*a*, 2011). In this study we have demonstrated the dynamics of the system, when the perturbation itself (not only its gradient) enters into the amplitude equation. It is shown that such a 'distortion' of the initial system, even being rather small, drastically changes its dynamics near the stability threshold in such aspects as selected patterns and direction of branching.

Similar phenomena can be expected in other systems. Taking into account weak non-Boussinesq effects, such as dependence of viscosity and other phenomenological coefficients on both the temperature and concentration, provides another valuable example of such a problem. A surface or interface deformation, when the layer thickness determines 'mobility' and other hydrodynamic properties of the system under consideration, also can be mentioned.

Acknowledgement

This work is partially supported by the European Union via FP7 Marie Curie scheme Grant PITN-GA-2008-214919 (MULTIFLOW).

Appendix A. Brief review for the case of no adsorption

Here, for the sake of convenience, we briefly present the main results of Oron & Nepomnyashchy (2004) and Shklyaev *et al.* (2007), which are necessary for the current problem. Recall that a different time scale and different signs of the Soret number and the concentration field were used in the cited papers.

The fast evolution (in the time $\tau = \epsilon^2 t$) of F and G, the primary parts of the temperature and concentration disturbances, is governed by (4.24).

For the monotonic mode ($\partial_\tau = 0$ at the stability boundary) this results in the following stability threshold:

$$m_0 = \frac{L}{L - \chi - \chi L}. \tag{A 1}$$

Nonlinear evolution of perturbations is governed by (4.10) with $k_{ad} = 0$.

The stability threshold for the oscillatory mode is

$$m_0 = \frac{1 + L}{1 - \chi} \tag{A 2}$$

https://doi.org/10.1017/jfm.2012.619 Published online by Cambridge University Press

and the frequency of the neutral oscillation in τ is given by ΩK^2,

$$\Omega^2 = \frac{\chi\left(1+L+L^2\right)-L^2}{1-\chi}. \tag{A 3}$$

The general solution of (4.24) for $h = F + G$ can be presented as

$$h = \sum_{\boldsymbol{K}} A_{\boldsymbol{K}}(\tau_2)\exp[\mathrm{i}(\boldsymbol{K}\cdot\boldsymbol{R} - \Omega K^2\tau)] + \text{c.c.}, \tag{A 4}$$

F and G can be expressed through h via (4.24).

Nonlinear evolution of the Fourier amplitudes $A_{\boldsymbol{K}}$ in slow time τ_2 is governed by the solvability conditions of the following linear non-homogeneous problem

$$\begin{aligned} L_1(Q,R) = {} & -\dot{F} - F - m_1\nabla^2 h - \frac{m_0}{60}\nabla^4\left[3\Phi - 2m_0\left(1-\chi-\frac{\chi}{L}\right)h\right] \\ & - \frac{m_0^2}{10}\nabla^2\left[\frac{1}{P}(\nabla h)^2 + 6\zeta\right] - \frac{m_0^2}{10}\left(1+\frac{2}{P}\right)\nabla\cdot(\nabla^2 h\nabla h) \\ & + \frac{48m_0^2}{35}\nabla\cdot[(\nabla h\cdot\nabla F)\nabla h] - \frac{312m_0^2}{35P}J(F,\psi), \end{aligned} \tag{A 5}$$

$$\begin{aligned} L_2(Q,R) = {} & -\dot{G} + \chi m_1\nabla^2 h + \frac{\chi m_0}{60}\nabla^4\left[3\Phi - 2m_0\left(1-\chi-\frac{\chi}{L}\right)h\right] \\ & + \frac{\chi m_0^2}{10}\nabla^2\left[\frac{1}{P}(\nabla h)^2 + 6\zeta\right] + \frac{\chi m_0^2}{10}\left(1+L^{-1}+\frac{2}{P}\right)\nabla\cdot(\nabla^2 h\nabla h) \\ & - \frac{48m_0^2}{35}\nabla\cdot\{[\nabla h\cdot\nabla(\chi F - L^{-1}G)]\nabla h\} - \frac{312m_0^2}{35P}J(G,\psi), \end{aligned} \tag{A 6}$$

where $Q(\boldsymbol{R},\tau,\tau_2) = \theta^{(2)}$, $R(\boldsymbol{R},\tau,\tau_2) = \Gamma^{(2)}$,

$$\zeta = \nabla h\cdot\nabla[(1-\chi)F + L^{-1}G], \tag{A 7}$$

$$\Phi = \left[2 + \frac{m_0}{P}(1-\chi)\right]h - \frac{1+\chi L}{P}F - \frac{L}{P}G, \tag{A 8}$$

$J(f,g) = f_X g_Y - f_Y g_X$ is a Jacobian of the mapping from (X,Y) to (f,g). The field ψ is determined by the following problem

$$\nabla^2\psi = h_Y\nabla^2 h_X - h_X\nabla^2 h_Y; \tag{A 9}$$

it coincides with the toroidal potential of the velocity field up to a constant factor.

At small supercriticality, each Fourier amplitude obeys the equation

$$\dot{A}_{\boldsymbol{K}} = \gamma^{(o)} A_{\boldsymbol{K}}, \tag{A 10}$$

where

$$\begin{aligned} \gamma^{(o)} = {} & -\frac{1}{2}\left(1 + \mathrm{i}\frac{L+\chi m_0}{\Omega}\right) + \frac{m_2 K^2}{2}\left(1-\chi-\mathrm{i}\frac{\chi - L + \chi L}{\Omega}\right) \\ & + \frac{m_0 K^4}{120P}\left(f + \mathrm{i}\frac{f_i}{\Omega}\right), \end{aligned} \tag{A 11}$$

$$f = -\chi[2P(L^{-1}-1+L) - 3(1+L)] + (2PL - 4P - 3L), \tag{A 12}$$

$$f_i = 2P(\chi - L + \chi L)[3 + m_0 L^{-1}(\chi - L + \chi L)] + 3(1-\chi)\Omega^2. \tag{A 13}$$

https://doi.org/10.1017/jfm.2012.619 Published online by Cambridge University Press

It is noteworthy to discuss briefly the branching on a square lattice, when h can be presented by (4.29). In this case the amplitudes of the leading Fourier harmonics are governed by (4.31) with

$$2K_0 = K_1 = 2(\alpha^{(o)} + \beta^{(o)}), \quad K_3 = 2\alpha^{(o)}, \tag{A 14a}$$

$$K_2 = \beta^{(o)} + \frac{\mu^{(o)}\mu_2^{(o)}}{\gamma_0^{(o)}(\sqrt{2}K_c) - 2\gamma_0^{(o)}(K_c)}, \tag{A 14b}$$

$$\alpha^{(o)} = \frac{24m_0^2K^4}{35L}\left(L + 1 + \mathrm{i}\frac{L^2 + 1 - m_0}{\Omega}\right), \quad \beta^{(o)} = -\frac{48m_0^2K^4}{35}\frac{\mathrm{i}}{\Omega}, \tag{A 14c}$$

$$\mu^{(o)} = \mu^{(1)} + \mu^{(2)}, \quad \mu_2^{(o)} = 2\mu^{(1)} + 2\mu^{(2)}\left(1 + 2P^{-1}\right), \tag{A 14d}$$

$$\mu^{(1)} = -\frac{m_0^2K^4\chi}{20L}\left(1 + \frac{\mathrm{i}}{\Omega}\right), \quad \mu^{(2)} = \frac{m_0^2K^4}{20}\left[1 - \chi - \frac{\mathrm{i}}{\Omega}(\chi - L - \chi L)\right]. \tag{A 14e}$$

Here $\gamma_0^{(o)}(K)$ is the growth rate exactly for the critical Marangoni number $m_2 = m_{2c}$. (Therefore, $\gamma_0^{(o)}(K_c)$ is pure imaginary, whereas $\mathrm{Re}\gamma_0^{(o)}(\sqrt{2}K_c) < 0$.) The term proportional to $\mu^{(o)}\mu_2^{(o)}$ in K_2 describes generation of the oblique waves $C_j (j = 1\text{–}4)$ and their feedback on the dynamics of the leading harmonics. This term is the only addition generated by quadratic nonlinearity (Pismen 1988; Shklyaev *et al.* 2007).

Appendix B. Coefficients of the amplitude equation (4.10)

The coefficients of (4.10) are

$$\bar{\gamma}_1 = \bar{\gamma}_0 m_2 + \frac{k_{ad}L_s\chi}{L}(1 + L^{-1}), \tag{B 1}$$

$$\bar{\gamma}_2 = \frac{1}{15}(1 - \chi - \chi L^{-1}), \tag{B 2}$$

$$\bar{\gamma}_3 = \frac{1}{5P}(1 - \chi - \chi L^{-1}) - \frac{\bar{\alpha}}{10}, \tag{B 3}$$

$$\bar{\gamma}_4 = \frac{1}{10P}(1 - \chi - \chi L^{-1}) - \frac{3}{5}\bar{\alpha}, \tag{B 4}$$

$$\bar{\gamma}_5 = \frac{48}{35}[1 - \chi(1 + L^{-1} + L^{-2} + L^{-3})], \tag{B 5}$$

$$\bar{\gamma}_6 = -\frac{312}{35P}\bar{\alpha}, \tag{B 6}$$

$$\bar{\gamma}_7 = 6\frac{k_{ad}\chi}{L}(1 + L^{-1}). \tag{B 7}$$

Recall, that $\bar{\gamma}_0 = (1 - \chi - \chi L^{-1})^2$ and $\bar{\alpha} = \chi(1 + L^{-1} + L^{-2}) - 1$.

REFERENCES

AGRAWAL, M. L. & NEUMAN, R. D. 1988 Surface diffusion in monomolecular films. *J. Colloid Interface Sci.* **121**, 366–380.

ANDOH, Y. & YASUOKA, K. 2007 Molecular understanding of dynamical properties of the vapor/ethanol-aqueous-solution interface. *Mol. Simulation* **33**, 139–145.

https://doi.org/10.1017/jfm.2012.619 Published online by Cambridge University Press

BERG, J. C. & ACRIVOS, A. 1965 The effect of surface active agents on convection cells induced by surface tension. *Chem. Engng Sci.* **20**, 737–745.

BERNOFF, A. J. 1988 Slowly varying fully nonlinear wavetrains in the Ginzburg–Landay equation. *Physica* D **30**, 363–381.

BERNOFF, A. J. & BERTOZZI, A. L. 1995 Singularities in a modified Kuramoto–Sivashinsky equation describing interface motion for phase transition. *Physica* D **85**, 375–404.

BLACKBURN, H. M., SHERWIN, S. J. & BARKLEY, D. 2008 Convective instability and transient growth in steady and pulsatile stenotic flows. *J. Fluid Mech.* **607**, 267–277.

CHEN, C. F. & CHEN, C. C. 1994 Effect of surface tension on the stability of a binary fluid layer under reduced gravity. *Phys. Fluids* **6**, 1482–1490.

CLUNE, T., DEPASSIER, M. C. & KNOBLOCH, E. 1996 Long wavelength oscillatory instability in binary fluids. In *Instabilities and Nonequilibrium Structures* (ed. E. Tirapegui & W. Zeller), pp. 75–84. Kluwer.

CRASTER, R. V. & MATAR, O. K. 2009 Dynamics and stability of thin liquid films. *Rev. Mod. Phys.* **81**, 1131–1198.

EDMONSTONE, B. D., MATAR, O. K. & CRASTER, R. V. 2006 A note on the coating of an inclined plane in the presence of soluble surfactant. *J. Colloid Interface Sci.* **293**, 222–229.

GOLDOBIN, D. S. & LYUBIMOV, D. V. 2007 Soret-driven convection of binary mixture in a horizontal porous layer in the presence of a heat or concentration source. *Sov. Phys. JETP* **104**, 830–836.

GOLOVIN, A. A., NEPOMNYASHCHY, A. A. & PISMEN, L. M. 1995 Pattern formation in large-scale Marangoni convection with deformable interface. *Physica* D **81**, 117–147.

GOLUBITSKY, M., SWIFT, J. W. & KNOBLOCH, E. 1984 Symmetries and pattern selection in Rayleigh–Bérnard convection. *Physica* D **10**, 249–276.

HAMID, A. S. A., KECHIL, S. A. & AZIZ, A. S. A. 2011 Marangoni instability in a fluid layer with insoluble surfactant. *World Acad. Sci. Engng Technol.* **58**, 24–28.

HOYLE, R. B. 2006 *Pattern Formation: An Introduction to Methods*. Cambridge University Press.

HURLE, D. T. J. & JAKEMAN, E. 1971 Soret-driven thermosolutal convection. *J. Fluid Mech.* **47**, 667–687.

JOHNSON, D. O. & STEBE, K. J. 1996 Experimental confirmation of the oscillating bubble technique with comparison to the pendant bubble method: the adsorption dynamics of 1-decanol. *J. Colloid Interface Sci.* **182**, 526–538.

KALITZOVA-KURTEVA, P., SLAVTCHEV, S. & ORON, A. 2009 Long-wavelength monotonic Marangoni instability in a binary mixture layer with nonlinear Soret effect. *J. Theor. Appl. Mech. (Sofia)* **39** (1), 31–54.

KOSTAREV, K. G., ZUEV, A. L. & VIVIANI, A. 2009 Experimental considerations of solutocapillary flow initiation on bubble/drop interface in the presence of a soluble surfactant. *Microgravity Sci. Technol.* **21**, 59–65.

KUMAR, N., COUZIS, A. & MALDARELLI, C. 2003 Measurement of the kinetic rate constants for the adsorption of superspreading trisiloxanes to an air/aqueous interface and the relevance of these measurements to the mechanism of superspreading. *J. Colloid Interface Sci.* **267**, 272–285.

LANDAU, L. D. & LIFSHITZ, E. M. 1987 *Fluid Mechanics*. Pergamon.

LEAL, L. G. 2007 *Advanced Transport Phenomena*. Cambridge University Press.

LEVICH, V. G. 1962 *Physicochemical Hydrodynamics*. Prentice-Hall.

LI, Z. X., LU, J. R., STYRKAS, D. A. & THOMAS, R. K. 1993 The structure of the surface of ethanol/water mixtures. *Mol. Phys.* **80**, 925–939.

LIN, S.-Y., LU, T.-L. & HWANG, W.-B. 1996 Adsorption kinetics of decanol at the air–water interface. *Langmuir* **11**, 555–562.

MACLEOD, C. A. & RADKE, C. J. 1994 Surfactant exchange kinetics at the air–water interface from the dynamic tension of growing liquid drop. *J. Colloid Interface Sci.* **166**, 73–88.

MATAR, O. K. & CRASTER, R. V. 2009 Dynamics of surfactant-assisted spreading. *Soft Matt.* **5**, 3801–3809.

MIKISHEV, A. B. & NEPOMNYASHCHY, A. A. 2010*a* Long-wavelength Marangoni convection in a liquid layer with insoluble surfactant: linear theory. *Microgravity Sci. Technol.* **22**, 415–423.

https://doi.org/10.1017/jfm.2012.619 Published online by Cambridge University Press

MIKISHEV, A. B. & NEPOMNYASHCHY, A. A. 2010*b* Nonlinear large-scale Marangoni convection in a heated liquid layer with insoluble surfactant. *Phys. Rev.* E **82**, 046306.

NEPOMNYASHCHY, A. A., GOLOVIN, A. A., GUBAREVA, V. & PANFILOV, V. 2004 Global feedback control of a long-wave morphological instability. *Physica* D **199**, 61–81.

NEPOMNYASHCHY, A. A. & SIMANOVSKII, I. B. 1986 Thermocapillary convection in two-layer systems in the presence of a surface active agent at the interface. *Fluid Dyn.* **21**, 169–174.

NEPOMNYASHCHY, A. A. & SIMANOVSKII, I. B. 1988 Occurrence of thermocapillary convection in a two-layer system in the presence of a soluble surfactant. *Fluid Dyn.* **23**, 302–306.

NEPOMNYASHCHY, A. A. & SIMANOVSKII, I. B. 1992 Excitation of thermal-capillary convection at a deformable interface in systems with a surface-active agent. *J. Appl. Mech. Tech. Phys.* **33**, 379–385.

ORON, A. & NEPOMNYASHCHY, A. A. 2004 Long-wavelength thermocapillary instability with the Soret effect. *Phys. Rev.* E **69**, 016313.

PALMER, H. J. & BERG, J. C. 1972 Hydrodynamic stability of surfactant solutions heated from below. *J. Fluid Mech.* **51**, 385–402.

PAN, R., GREEN, J. & MALDARELLI, C. 1998 Theory and experiment on the measurement of kinetic rate constants for surfactant exchange at an air/water interface. *J. Colloid Interface Sci.* **205**, 213–230.

PEARSON, J. R. A. 1958 On convection cells induced by surface tension. *J. Fluid Mech.* **4**, 489–500.

PENFOLD, J., RICHARDSON, R. M., ZARBAKHSH, A., WEBSTER, J. R. P., BUCKNALL, D. G., RENNIE, A. R., JONES, R. A. L., COSGROVE, T., THOMAS, R. K., HIGGINS, J. S., FLETCHER, P. D. I., DICKINSON, E., ROSER, S. J., MCLURE, I. A., HILLMAN, A. R., RICHARDS, R. W., STAPLES, E. J., BURGESS, A. N., SIMISTERO, E. A. & WHITEP, J. W. 1997 Recent advances in the study of chemical surfaces and interfaces by specular neutron reaction. *J. Chem. Soc. Faraday Trans.* **93**, 3899–3917.

PISMEN, L. 1988 Selection of long-scale oscillatory convective patterns. *Phys. Rev.* A **38**, 2564–2572.

PODOLNY, A., ORON, A. & NEPOMNYASHCHY, A. A. 2005 Long-wave Marangoni instability in a binary-liquid layer with deformable interface in the presence of Soret effect: linear theory. *Phys. Fluids* **17**, 104104.

PODOLNY, A., ORON, A. & NEPOMNYASHCHY, A. A. 2006 Linear and nonlinear theory of longwave Marangoni instability with the Soret effect at finite Biot numbers. *Phys. Fluids* **18**, 054104.

RAINA, G., KULKARNI, G. U. & RAO, C. N. R. 2001 Mass spectrometric determination of the surface compositions of ethanolwater mixtures. *Int. J. Mass Spectrometry* **212**, 267–271.

ROBERTS, M., SWIFT, J. W. & WAGNER, D. H. 1986 The Hopf bifurcation on a hexagonal lattice. In *Multiparameter Bifurcation Theory* (ed. M. Golubitsky & J. Guckenheimer), *Contemp. Math.*, vol. 56, pp. 283–318. American Mathematical Society.

RYABITSKII, E. A. 1993 Oscillatory thermocapillary instability of a liquid layer in the presence of a surfactant. *Fluid Dyn.* **28**, 3–6.

RYABITSKII, E. A. 1996 Thermocapillary instability of a liquid layer in the presence of a soluble surfactant. *Fluid Dyn.* **31**, 1–5.

RYABITSKII, E. A. 2000 Thermocapillary instability of a liquid layer with allowance for the Soret effect. *Fluid Dyn.* **35**, 315–320.

SCRIVEN, L. E. & STERNLING, C. V. 1964 On cellular convection driven by surface-tension gradients: effects of mean surface tension and surface viscosity. *J. Fluid Mech.* **19**, 321–340.

SHIN, J. Y. & ABBOTT, N. L. 2001 Combining molecular dynamics simulations and transition state theory to evaluate the sorption rate constants for decanol at the surface of water. *Langmuir* **17**, 8434–8443.

SHKLYAEV, S. & NEPOMNYASHCHY, A. A. 2011 Marangoni instability of a heated liquid layer in the presence of a soluble surfactant. Oscillatory mode for small Lewis number. *Eur. Phys. J.* ST **192**, 155–161.

https://doi.org/10.1017/jfm.2012.619 Published online by Cambridge University Press

SHKLYAEV, S., NEPOMNYASHCHY, A. A. & ORON, A. 2007 Three-dimensional oscillatory long-wave Marangoni convection in a binary liquid layer with the Soret effect: bifurcation analysis. *Phys. Fluids* **19**, 072105.

SHKLYAEV, S., NEPOMNYASHCHY, A. A. & ORON, A. 2009*a* Long-wave oscillatory convection in a binary liquid: hexagonal patterns. *Europhys. Lett.* **86**, 14005.

SHKLYAEV, S., NEPOMNYASHCHY, A. A. & ORON, A. 2009*b* Marangoni convection in a binary liquid layer with Soret effect at small Lewis number: linear stability analysis. *Phys. Fluids* **21**, 054101.

SHKLYAEV, S., NEPOMNYASHCHY, A. A. & ORON, A. 2011 Oscillatory long-wave Marangoni convection in a layer of a binary liquid: hexagonal patterns. *Phys. Rev.* E **84**, 056327.

SILBER, M. & KNOBLOCH, E. 1991 Hopf bifurcation on a square lattice. *Nonlinearity* **4**, 1063–1106.

SIVASHINSKY, G. I. 1983 On cellular instability in the solidification of a dilute binary alloy. *Physica* D **8**, 243–248.

SLAVTCHEV, S., KALITZOVA-KURTEVA, P. & ORON, A. 2009 Long-wavelength oscillatory Marangoni instability in a binary mixture layer with nonlinear Soret effect. *J. Theor. Appl. Mech. (Sofia)* **39** (3), 63–78.

SMITH, K. A. 1966 On convective instability induced by surface-tension gradients. *J. Fluid Mech.* **24**, 401–414.

TAREK, M., BANDYOPADHYAY, S. & KLEIN, M. L. 1998 Molecular dynamics studies of aqueous surfactants systems. *J. Molecular Liquids* **78**, 1–6.

VALKOVSKA, D. S. & DANOV, K. D. 2000 Determination of bulk and surface diffusion coefficients from experimental data for thin liquid film drainage. *J. Colloid Interface Sci.* **223**, 314–316.

VANHOOK, S. J., SCHATZ, M., SWIFT, J. B., MCCORMICK, W. D. & SWINNEY, H. L. 1997 Long-wavelength surface-tension-driven Bénard convection: experiment and theory. *J. Fluid Mech.* **345**, 45–78.

VIDAL, A. & ACRIVOS, A. 1966 Nature of the neutral state in surface-tension driven convection. *Phys. Fluids* **9**, 615–616.

YIANTSIOS, S. G. & HIGGINS, B. G. 2010 A mechanism of Marangoni instability in evaporating thin liquid films due to soluble surfactant. *Phys. Fluids* **22**, 022102.

https://doi.org/10.1017/jfm.2012.619 Published online by Cambridge University Press